Phylogenomics, life history and morphological evolution of ophiocomid brittlestars

Timothy D. O'Hara, Andrew F. Hugall, Paula A. Cisternas, Emilie Boissin, Guadalupe Bribiesca-Contreras, Javier Sellanes, Gustav Paulay, Maria Byrne

HIGHLIGHTS:

- Definitive phylogeny of the Ophiocomidae inferred from 39 species and 258 kbp DNA.
- New ophiocomid classification proposed with four extant genera aged 30-60 my.
- Lecithotrophy has evolved only in the polymorphic genus *Ophiomastix*.
- Elevated allelic heterozygosity occurs in the asexual *Ophiocomella* species-complex.
- Mitochondrial gene-order rearrangements are evident within *Ophiomastix.*

Ontogeny

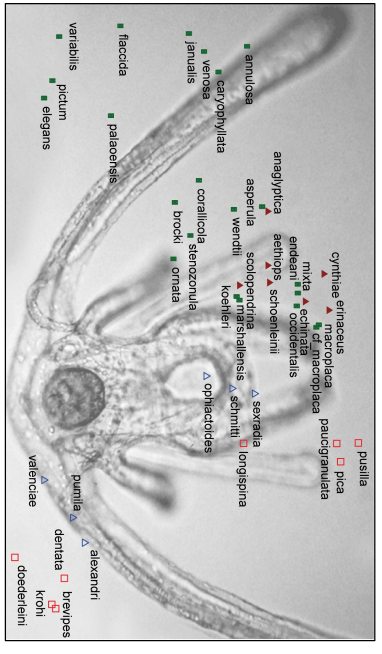

Diversity

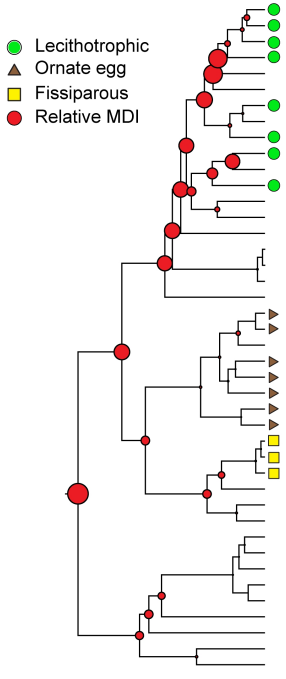

Taxonomy

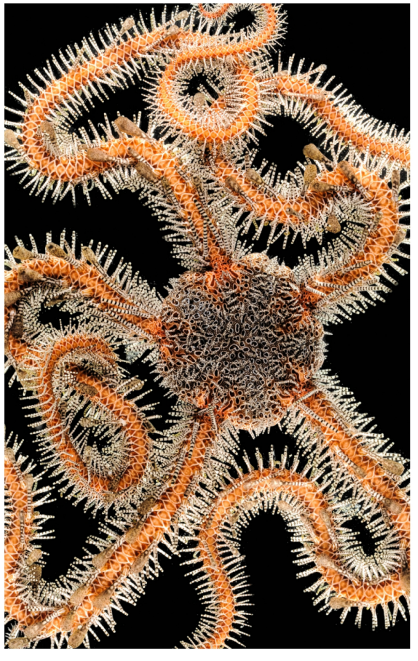

Genomics

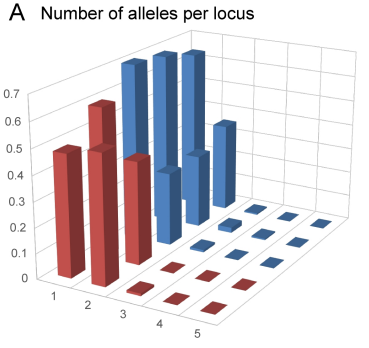

Phylogenomics, life history and morphological evolution of ophiocomid brittlestars

Timothy D. O'Hara [a], Andrew F. Hugall [a], Paula A. Cisternas [b], Emilie Boissin [c], Guadalupe Bribiesca-Contreras [a,d], Javier Sellanes [e], Gustav Paulay [f], Maria Byrne [b]

[a] *Museums Victoria, Sciences Department, GPO Box 666, Melbourne, 3000, Australia*

[b] *University of Sydney, School of Medicine, Discipline of Anatomy and Histology, 2006, Australia*

[c] *PSL Research University: EPHE-UPVD-CNRS, USR 3278 CRIOBE, Université de Perpignan, Laboratoire d'Excellence CORAIL, 52 Avenue Paul Alduy, 66860 Perpignan Cedex, France*

[d] *University of Melbourne, Biosciences, 3010, Australia*

[e] *Universidad Católica del Norte, Departamento de Biologia Marina, Coquimbo, Chile*

[f] *University of Florida, Florida Natural History Museum, Gainesville, USA*

ABSTRACT

Brittle-stars in the family Ophiocomidae are large and colourful inhabitants of tropical shallow water habitats across the globe. Here we use targeted capture and next-generation sequencing to generate robust phylogenomic trees for 39 of the 43 species in order to test the monophyly of existing genera. The large genus *Ophiocoma*, as currently constituted, is paraphyletic on our trees and required revision. Four genera are recognised herein: an expanded *Ophiomastix* (now including *Ophiocoma wendtii*, *O. occidentalis*, *O. endeani*, *O. macroplaca*, and *Ophiarthrum* spp), *Ophiocomella* (now including the non-fissiparous *Ophiocoma pumila*, *aethiops* and *valenciae*) and *Breviturma* (now including *Ophiocoma pica*, *O. pusilla*, *O. paucigranulata* and *O. longispina*) and a restricted *Ophiocoma*. The resulting junior homonym *Ophiomastix elegans* is renamed *O. brocki*. The genus *Ophiomastix* exhibits relatively high rates of morphological disparity compared to other lineages. *Ophiomastix flaccida* and *O.* (formerly *Ophiarthrum*) *pictum* have divergent mitochondrial genomes, characterised by gene-order rearrangements, strand recoding, enriched GT base composition, and a corresponding divergence of nuclear mitochondrial

protein genes. The new phylogeny indicates that larval and developmental transitions occurred rarely. Larval culture trials show that species with abbreviated lecithotrophic larval development occur only within *Ophiomastix*, although the possible monophyly of these species is obscured by the rapid early radiation within this genus. Asexual reproduction by fission is limited to one species-complex within *Ophiocomella*, also characterised by elevated rates of allelic heterozygosity, and which has achieved a relatively rapid global distribution. The crown ages of the new genera considerably predate the closure of the Tethyan seaway and all four are distributed in both the Atlantic and Indo-Pacific Oceans. Two species pairs appear to reflect the closure of the Panama Seaway, although their fossil-calibrated node ages (12-14 ± 6 my), derived from both concatenated sequence and multispecies coalescent analyses, considerably predate the terminal closure event. *Ophiocoma erinaceus* has crossed the East Pacific barrier and is recorded from Clipperton Island, SW of Mexico.

KEYWORDS:
Ophiuroidea, Ophiocomidae, Exon-capture, larval development, asexual reproduction

HIGHLIGHTS:

- Definitive fossil calibrated phylogeny of the brittle-star family Ophiocomidae inferred from 39 species and 1465 exon (257kbp) + COI/16S mtDNA data-matrix, superimposed with morphological, life history and biogeographic traits.
- New phylogenetic-based classification proposed for the Ophiocomidae with four extant genera aged 30-60 my.
- Life history transitions have occurred rarely within the Ophiocomidae.
- Mitochondrial gene-order rearrangements evident within *Ophiomastix.*
- Elevated allelic heterozygosity found in the faculatively asexual *Ophiocomella* species-complex

1. Introduction

The brittle-star family Ophiocomidae contains large colourful species (Figure 1) that are abundant on and around coral reefs in all tropical regions, often dominating the echinoderm cryptofauna. Ophiocomids have broad ecological niches, various feeding mechanisms (from suspension-deposit to scavenge feeding) and contrasting life histories, including species with

planktonic feeding and non-feeding larval development, and fissiparous species capable of both sexual and asexual reproduction (Mladenov and Emson 1984, Cisternas et al. 2004, Fourgon et al. 2005, Oak and Scheibling 2006). Intriguing behaviours include 'babysitting' other species in the bursae (Hendler et al. 1999b, Fourgon et al. 2007), and the ability to change skin colour for camouflage and to facilitate negative phototaxis under a range of light intensities (Hendler 1984, O'Hara et al. 2004). Several Caribbean species have extensive networks of putative dermal photoreceptors on the external surface of arm plates (Sumner-Rooney et al. 2018).

Despite this interest, the evolutionary relationships and taxonomy of the ophiocomids have been problematic. The traditional understanding of the family dates from 1915, when the insightful Japanese scientist Hikoshichirô Matsumoto (1915) defined it as including species with a cluster (> 2) of well-developed dental papillae placed at the ventral apex of each jaw in addition to several oral papillae on each jaw side (Fig. 1G). However, analyses of SEM imagery (Martynov 2010, Thuy and Stöhr 2016) and molecular data (O'Hara et al. 2017) have resulted in the progressive removal of unrelated but morphologically convergent genera, including *Ophiopsila* (now in the Ophiopsilidae), *Clarkcoma* (Clarkcomidae), *Ophiopteris* (Ophiopteridae) and *Ophiocomina* (Ophiotomidae). The Ophiocomidae is thus now restricted to four genera; *Ophiocomella* (3 species), *Ophiocoma* (22), *Ophiomastix* (15), and *Ophiarthrum* (3). *Ophiocomella* contains three 6-armed, fissiparous species, whereas the other three genera are distinguished by the disc armament, formed primarily from granules (*Ophiocoma*), spines (at least 2x high as wide; *Ophiomastix*) or naked skin (*Ophiarthrum*) respectively. The composition of *Ophiocoma* continues to be a problem; Devaney (1970) defined four informal groups of species on the basis of morphology but genetic data (O'Hara et al. 2017) indicates that these may not be monophyletic. Convergent evolution is a major problem for morphological systematics, which still dominates genus-level taxonomy across the Ophiuroidea. Frequently, a hierarchy has been erected based on a few obvious morphological characters without any data on the homology or polarity of these characters.

Ophiocomids exhibit considerable variation in life history characteristics, including the presence of smooth or ornate fertilisation envelopes around eggs (Cisternas et al. 2013), feeding planktotrophic ophiopleuteus larvae or non-feeding lecithotrophic vitellaria larvae (Cisternas et al. 2004, Fourgon et al. 2005, Delroisse et al. 2013) (e.g. Fig. 1 C-D), and the addition of asexual reproduction by fission in a few species (Mladenov and Emson 1984)

(e.g. Fig.1 F). Of these, the transition from planktotrophy to lecithotrophy has received the most attention. The ancestor of the class Ophiuroidea is assumed to have had an ophiopleuteus larva that transforms into a lecithotrophic larva just before metamorphosis (McEdward and Miner 2001). The shift from planktotrophy to lecithotrophy can then occur through the increased maternal provisioning of the embryo followed by progressive simplification then loss of larval feeding structures. This shift appears to have happened repeatedly across the Ophiuroidea (McEdward and Miner 2001) including the Ophiocomidae (Mladenov 1985, Cisternas et al. 2004). Asexuality is often associated with unusual patterns of genetic diversity and hybrid origins (Birky 1996).

Here we investigate phylogenetic relationships and the evolution of morphological and life history characters within the Ophiocomidae. To this end, we utilized the next-generation sequencing exon-capture system described in Hugall et al. (2016) to generate multi-locus data for as many Ophiocomidae species as were available. Briefly, this exon-capture system is based on 425 orthologous genes (448kbp) determined from a transcriptome phylogenetic study across the class (O'Hara et al. 2014). These genes were used to develop an exon-capture system designed to capture, filter and assemble 1552 exons (285kbp) from museum material (Hugall et al. 2016, O'Hara et al. 2017). We also utilised a tapestry approach to add samples from a few species for which we have only legacy mtDNA (COI, 16S) data from Sanger sequencing. The resulting multi-locus and supermatrix data is used to test the monophyly of existing genera, to explore the biogeography of the group, and to correlate life-history with taxonomic, genetic and morphological diversity.

2. Methods

2.1. Sequence data

The phylogenomic dataset used here was derived using our exon-capture system (O'Hara et al. 2014, Hugall et al. 2016, O'Hara et al. 2017). The multi-stage strategy is described in detail in Hugall et. al. (2016), and further information on loci, pipeline scripts and data, can be found in DRYAD packages http://dx.doi.org/10.5061/dryad.rb334 and http://dx.doi.org/10.5061/dryad.db339, with information specific to this paper in [*to be confirmed*]. Library preparation, hybrid enrichment and next generation sequencing were all

done through commercial laboratories (Georgia Genomics Facility, Atlanta, Georgia, USA and Arbor Biosciences, Ann Arbor, Michigan, USA).

For this study we obtained 14-98% of our target from 46 samples (including one transcriptome *O. wendtii*) of 37 nominal species across the Ophiocomidae, as restricted by O'Hara et al. (2017) and 2 exon-capture outgroup species (Table S1). Several species (*O. dentata*, *O. elegans* Brock, *O. erinaceus*, *O. longispina*, *O. sexradia, O. venosa*) were represented by more than one sample due to taxonomic uncertainty or to test extensive distributional ranges. We excluded the nuclear fragments of *Ophiocomella schmitti* as coverage was very low (14%). For all samples, reads were de-duplicated and trimmed (scripts RDUPE and BULK), mapped using the de novo assembled super-reference method (scripts TASSER and TASSMAP) with a minimum coverage limit of 5 and per-sample exclusion of exons with excess polymorphism (script HEXER). Alignment is built into the read mapping, with all exons kept in-frame (Hugall et al. 2016). We then further trimmed the dataset by removing codons adjacent to exon boundaries or with <50% of taxa (script TEFORM1), resulting in a dataset of 256,509 sites in 1465 exons in 416 genes, 91 % data-complete (range 25-99%, median 93%).

In addition we obtained mitochondrial sequences from either our exon-capture system (1432 bp COI built into the exon-capture target, and occasionally 16S from off-target reads) or through dedicated Sanger sequencing (16S, COI). For Sanger sequencing, universal primers, 16Sar and 16sbr (Palumbi et al. 1991) were used to obtain approximately 560 bp of the 3' end of 16S, trimmed to 440bp after removal of ambiguous regions. The 'barcode' primers (Ward et al. 2008) were used to sequence 655bp of COI of 'Ophiocoma' *macroplaca*. These sequences enabled us to incorporate a further three species for which we only had mitochondrial data, *O. anaglyptica* (16S), *O. macroplaca* (COI) and *Ophiocomella schmitti* (COI), through a super-matrix approach (de Queiroz and Gatesy 2007). In all, we obtained molecular data from all recognised ophiocomid species except the rare *Ophiarthrum lymani*, *Ophiomastix corallicola*, *O. marshallensis* and *O. ornata*. *Ophiocomella caribbaea* is here recognised as a synonym of *O. ophiactoides* (following Parslow and Clark 1963) and *Ophiocoma aegyptica* a synonym of *pusilla* (following Olbers and Samyn 2012).

2.2. Phylogenetic analyses

2.2.1. Phylogenetic inference

Maximum Likelihood (ML) trees were inferred via RAxML v8.1.2 (Stamatakis 2014) with the GTR+Γ model of substitution, using the -f a function (100 fast bootstraps and 10 slow ML searches) to determine topology, with support assessed from 200 thorough bootstraps (-f i function). Two concatenated datasets were used: 1) a three codon-position partitioned dataset derived from nuclear DNA only, and 2) a four partition super-matrix dataset, including the three nuclear codon positions and a combined mitochondrial partition (16S+COI).

For species-tree analyses (Degnan and Rosenberg 2009, Lanier and Knowles 2012, Mirarab et al. 2014), we excluded *Ophiocomella schmitti* and *Ophiomastix janualis* due to low coverage, and selected genes with the following characteristics: at least 80% of taxa with at least 50% of sites and at least 50 variable nucleotide sites. This resulted in a set of 310 genes, with median 44 taxa per gene and median 303 genes per taxon. Nucelotide gene trees were estimated using RAxML (GTR+Γ model, with -f d ML search function), and a species tree inferred using ASTRAL-II v4.10.2 (Mirarab and Warnow 2015) using local posterior probabilities (LPP) as a measure of clade support (Sayyari and Mirarab 2016).

2.2.2. Bayesian phylogenetic dating

Chronograms were produced by Bayesian inference on the four partition (exon codon position and 16S/COI) super-matrix dataset using BEAST v2.4.6.0 (Bouckaert et al. 2014), with an HKY+ Γ substitution model (per partition, unlinked), uncorrelated lognormal rate relaxed-clock model, and birth-death speciation prior. The starting tree was set to RAxML topology. We used the only available fossil calibration for the group plus three TMRCA priors secondarily derived from our larger fossil-calibrated analysis of the higher systematics of the class (O'Hara et al. (2017): the root (Ophiodermatina: normal prior, mean=170, SD=10 my), outgroup taxa (Ophiodermatidea: normal prior, mean 130 my, SD 6 my) and the extant Ophiocomidae (gamma prior, alpha=5, beta=3, 80my offset fossil minimum constraint, giving median 92 my and 95% CI 83-113 my). Two independent 50M step chains were run

with 1/10000 sampling, and 20% burnin. Runs converged on the same topology and median likelihood and were combined to give a total 8000 posterior samples with ESS>300.

To test whether our recent node ages were overestimated through the use of concatenated sequence data (Ogilvie et al. 2017), we compared relative node heights of the species tree generated from concatenated data using BEAST (see above) to that generated from a Bayesian multispecies coalescent analysis using StarBEAST2 (Ogilvie et al. 2017). This latter methodology is best served by multiple alleles per taxon, which we obtained by explicit phasing from mapped reads, applying a minimum coverage of 8 and site state frequency limit of 0.20 for site base calling (ALLSEP pipeline, Hugall et al. 2016). We selected one hundred exons with the following characteristics: all taxa with >0.50 of sites per locus, minimum 40 variable sites per locus, complete phasing, and unlinked (i.e. only one exon per gene); amounting to 35kb sites, 99% complete. A slightly smaller taxon dataset (deleting low coverage samples *O. janualis, O. asperula* and *O. schmitti*) and simpler model were used for StarBEAST to ensure stable multi-locus coalescence analysis. The data were run on BEAST version 2.4.6.0 using the StarBEAST2 module, applying a HKY+Γ sequencing model (linked across loci), integrated analytical population size, lognormal relaxed clock, Yule speciation model, and the same calibrations as above (enforcing monophyly of the calibration nodes and the four major ingroup clades). The MCMC chain was run for 400 million steps, sampling 1/20000, with a 25% burnin, leaving 15,000 posterior samples (with ESS>150) for median MCC consensus species tree, as well as individual gene trees.

2.2.3. Allelic diversity in Ophiocomella

Due to its fissiparous asexual reproductive mode and striking result in the StarBEAST analysis (see results section), we further investigated allelic diversity within *Ophiocomella.* We evaluated both the number of, and divergence between, alleles per locus for 2 samples from fissiparous species (*O. sexradia* and *O. ophiactoides*) and 3 samples from non-fissiparous species (*O. valenciae*, *O. alexandri* and *O. pumila*). This used the phased data analysed per gene by custom exon-capture pipeline scripts. Number of alleles (an indication of ploidy) was estimated on the basis of the number of distinct sequence types among reads within a 120 base central section of each exon, with each read having >100 bases in this section. A sequence type was scored if it represented at least 10% of the reads with a total

coverage >30. Within sample allelic divergence was measured as the distance between alleles per gene (i.e. proportion of heterozygous sites in >100 bases). Bi-allelic genotypes were recorded for one randomly chosen SNP per gene with no missing data (349 loci). Expected heterozygosity (*He*) per locus was based on simple binomial expectations.

2.2.4. Mitochondrial genes in 'Ophiarthrum'

A putative mitochondrial genome for *Ophiomastix flaccida* was *de novo* assembled from off-target exon-capture reads using Trinity r20140717 (Grabherr et al. 2011). BLAST searches (Altschul et al. 1997) of the exon-capture read assembly confirmed that this contig of 16,747 bases was the only one containing mitochondrial-like genes and was closest to ophiuroid mtDNA sequences. Combined with GenBank ophiuroid mitogenomes (Table S4), provisional gene order was assessed via MITOS (http://mitos.bioinf.uni-leipzig.de/index.py, Bernt et al. 2013b). Gene order differences among mitogenomes were assessed using the CREx common interval rearrangement explorer, and summarized by principle coordinates analysis (PCoA using 'pcoa' function in R package APE v5.0) of a breakpoints and reversals distance matrix. Mitochondrial COI base content difference among Ophiocomidae and outgroups (46 taxa) was summarized by PCoA of Euclidian base composition distance matrix. The optimized model and ML tree were determined using IQTree v1.6.1 (Nguyen et al. 2015).

To investigate the effects of mitogenome evolution on nuclear gene divergence rates, we inferred RAxML amino acid phylogenies for exon-capture gene sets separated into general cytosolic protein genes (n=292, 63513 codons excluding ribosomal genes) and nuclear encoded mitochondrion protein genes (N-mt genes; n=56, 11113 codons). We did this using both combined data with partition branch lengths unlinked, and also as entirely separate data subsets. Relative branch lengths in the different classes of gene were then compared to investigate if changes in the rate of N-mt genes correlated with mitogenome evolution. Analyses used the JTT+ Γ +F model (optimally selected via IQTree v1.6.1, Nguyen et al. 2015). Numbers of amino acid differences per locus between selected taxa were summarized by partition. Gene type followed the transcriptome annotations of O'Hara et al. (2014) based on orthology with *Strongylocentrotus* and *Danio* genomes.

2.3. Adult morphological characters

Thirty morphological characters were assessed for 41 taxa either from examination of adult preserved specimens in Museum Victoria or from the literature (Table S2). The characters were primarily selected from external characters used in traditional taxonomy or internal ones from the work of Devaney (1968, 1970, 1978). A distance matrix was created using the Gower metric, from normalised quantitative characters and categorical binary/ordinal characters, using the daisy() function in the R package cluster 2.0.6 (Maechler et al. 2017). The distance matrix was ordinated using the pcoa() function in the R package ape 5.0 (Paradis et al. 2004), with negative eigenvectors corrected using the 'cailliez' method. The number of axes (n=5) was determined visually using the screeplot() function.

A measure of within-clade morphological variation was calculated for each internal node on the same tree using the relative Morphological Disparity (MDI) and subclade indices of Harmon et al. (2003) as implemented in the R library Geiger (Harmon et al. 2008). We used the five PCoA components rather than the morphological matrix to generate the MDI in order to avoid missing data. MDI close to one indicates that descendent subclades retain a considerable amount of the morphological variation, whereas values close to zero indicate that one subclade is morphologically divergent from the other, i.e. morphological disparity is partitioned between subclades. We refrained from utilising more complex macro-evolutionary analyses on this single family, preferring to await comparative approaches across the entire class Ophiuroidea.

2.4. Life history characters

Egg size and colour were determined from gravid ovaries in live and preserved specimens. Males and females were induced to spawn by varying light and temperature (Selvakumaraswamy and Byrne 2000) and some resulting fertilised eggs were preserved in 2% paraformaldehyde/0.2 μm filtered seawater for examination (Cisternas et al. 2013). In preserved specimens, developmental type was inferred from egg size following Sewell & Young (1997). Larvae were reared by standard echinoderm culturing methods (Strathmann 1987). These observations were supplemented by data in previous publications (Table 1).

297 **3. Results**

298

299 *3.1. Phylogenomics*

300

301 We obtained 1 transcriptome, 45 exon-capture samples (256,509 bp of nuclear exons plus
302 1431 bp of COI), and 26 mitochondrial (23x 440 bp 16S and 1x 656 bp COI) sequences from
303 Sanger sequencing, from 39 (91 %) of the recognised 43 species and 4 putatively undescribed
304 species of Ophiocomidae plus two outgroup taxa (Table S1). We obtained more than 75% of
305 our exon-capture target, except for three species, *asperula* (58%), *janualis* (24%) and *schmitti*
306 (14%) (Table S1).

307

308 *3.1.1. Phylogenetic topology*

309

310 The RAxML (Maximum Likelihood) analysis of the nuclear phylogenomic data (Fig. S5)
311 returned a topology with generally high bootstrap support (only nine internal nodes with less
312 than 100% support). The ASTRAL-II species-tree (for 43 exon-data taxa) returned similar
313 topology and relative support (ten nodes not fully supported) as the concatenated data tree
314 (Fig. S6). The topology differed only in the position of 'Ophiocoma' *wendtii* which shifted
315 from being sister to all *Ophiomastix* (RAxML) to sister to the *O. macroplaca* group
316 (ASTRAL-II). The crown *Ophiomastix* radiation contained a series of short internodes and
317 nodes with equivocal support. In addition to the uncertain position of *O. wendtii*, the position
318 of the *Ophiomastix variabilis*/*palaoensis* clade varied amongst the RAxML bootstraps and
319 gene-trees from between being 1) sister to the *O. pictum-elegans-flaccida* clade to 2) sister to
320 the majority of *Ophiomastix* species (*mixta-caryophyllata*). The 'Ophiocoma' *pica* terminal
321 was placed as sister to the *O. pusilla-longispina* clades on many bootstraps but was decisively
322 placed as sister to the *O. brevipes-paucigranulata* clade on the ASTRAL species tree (LPP
323 =100). Equivocal nodes were reduced to polytomies on the final topology (Fig. 2).

324

325 The addition of three species (*anaglyptica*, *macroplaca*, *schmitti*), with only mtDNA using
326 a supermatrix approach, resulted in lower apparent RAxML bootstrap values (Fig. S7) but
327 this was due entirely to instability in these additional taxa around the underlying exon data
328 backbone (e.g. same as Figure S1). In particular, the topological position of *anaglyptica*
329 (represented by only 384 bp of 16S) varied across bootstraps, although always within the
330 *Ophiocoma scolopendrina*-clade of species.

331

332 *3.1.2. Phylogenetic dating*

333

334 The BEAST2 supermatrix analysis (Fig. 3) resulted in the same topology as the
335 concatenated RAxML (Fig. S7). Only nodes around the three mtDNA-only taxa showed any
336 topological uncertainty. The variation in estimated node age was considerable, with the 95%
337 CI being on average 40% of node height for the major clades. The estimated age of the
338 separation between pairs of species (*Ophiocoma echinata-aethiops, O. pumila-alexandri*) on
339 either side of the Panama isthmus ranged from 12-14 ± 6 my. The separation is less clear cut
340 within the *Ophiocomella ophiactoides-schmitti-sexradia* clade, as the topological position of
341 *O. schmitti* varied (from the eastern Pacific, with only COI data in our tree). The relative
342 node heights of the older two cross-Panama species-pairs were broadly the same for a tree
343 based concatenated data (BEAST2) and a multispecies coalescent-based species tree
344 (StarBEAST2) (12-14 my vs 13-14 my; Fig. S8) indicating there these ages were not elevated
345 due to concatenating data.

346

347 *3.1.3. Fissiparous genomic diversity*

348

349 Estimates of node height between BEAST2 and StarBEAST2 trees substantially differed
350 only for the fissiparous *Ophiocomella ophiactoides-sexradia* species pair
351 (coalescent/concatenation 4.9 vs 0.4 my, ratio <0.2, Fig. S8). This was investigated further by
352 analysis of the underlying allelic diversity in these samples (*ophiactoides and sexradia*) and
353 related obligate sexual taxa (*alexandri, pumila* and *valenciae*) (Mladenov and Emson 1990).
354 There was no evidence of more than two alleles per locus, suggesting the nuclear genome is
355 diploid (Fig. 4a) but there was notably higher allele divergence in the fissiparous samples
356 compared to closely related taxa (Fig. 4b; median 0.015 vs 0.008). For many gene trees,
357 alleles clustered closer to an allele in the other fissiparous species rather than from its
358 corresponding chromosome (Fig. 4c; only 18% gene trees had reciprocally monophyletic
359 alleles). We ruled out paralogy as negligible because 1) of the multi-stage paralog filtering in
360 the exon-capture system, 2) there was no evidence for more than two alleles, and 3) in 80%
361 of gene trees alleles were monophyletic to the fissiparous clade. The small sample size (3)
362 precludes detailed analysis of Hardy-Weinberg expectations by locus but integrating across
363 the 349 loci SNP data suggests an overall substantial excess heterozygosity (cumulative
364 *Ho*=476, *He*=393; Chi^2 $p<10^{-7}$), consistent with asexual/hybrid origins (Balloux et al. 2003,

Ament-Velasquez et al. 2016). There was no evidence however for elevated *dN/dS* ratio in the fissiparous samples compared to related species (*alexandri, pumila and valenciae*; average *dN/dS* 0.051 versus 0.059). Across all available fissiparous samples (5 in three nominal species) COI diversity was π=0.0098.

3.1.4. Divergent COI

Mitochondrial COI and 16S genes in sister taxa *Ophiomastix flaccida* and 'Ophiarthrum' *pictum* appeared highly divergent. Fortuitous assembly of near-complete *O. flaccida* mitogenome indicated considerable differences in gene order (Fig. 5a), with COI and 16S likely being coded on the opposite strand relative to other ophiuroids. Both *O. flaccida* and *O. pictum* also showed considerable differences in COI base content, being much more GT-rich (65% vs 46%; Fig. 5b). This is consistent with observations on mitogenome strand bias and base-composition shifts (Bernt et al. 2013a), contributing to the observed greater sequence difference (0.38 vs 0.19 average among lineages), which is then exacerbated by optimal ML models (driving estimated divergences >>1; leading to aberrant placement in ophiuroid mitochondrial gene trees, Fig. 5c). Phylogenies of amino acid sequences of nuclear encoded general cytosolic and N-mt protein genes returned essentially the same topology, but indicated a 3x increase in the level of divergence in N-mt proteins versus general cytosolic proteins in *flaccida* and *pictum* (Fig. 5d). Amino acid p-distance per N-mt locus between these taxa and related species (*O. variabilis*, *O. mixta* and *O. occidentalis*) was consistently higher than within the latter group (median 0.033 vs 0.019), indicating a consistent signal across many loci.

3.2. Taxonomy

The inferred topology of the Ophiocomidae indicated that three of the four existing genera are not monophyletic (Fig. 2). In particular, *Ophiocoma*, as currently defined, comprised several paraphyletic clades, spanning such genera as *Ophiomastix, Ophiarthrum* and *Ophiocomella*. Thus a genus-level revision of the family was required. Our phylogeny contained four major clades that were good candidates for being considered genera. These clades had unequivocal support, were phylogenetically distinct (i.e. have long stems) and partitioned a significant proportion of the morphological and life-history diversity (Fig. 6 and

see below). Moreover, they showed some similarity to the informal species-groups within *Ophiocoma* proposed by Devaney (1970).

The first group contained all species currently considered to belong to the genus *Ophiomastix* plus *Ophiarthrum* and several of the scolopendrina-group of *Ophiocoma* species (*endeani*, *macroplaca*, *occidentalis*, *wendtii*). This expanded *Ophiomastix* contained considerable morphological and developmental diversity (see below), however, the short internodes and lack of node support within this clade precluded further subdivision based on our data (Fig. 2). The informal subdivision of *Ophiomastix* proposed by Devaney (1978) was not supported. The traditional separation of *Ophiathrum* from *Ophiomastix* was based on a single character, the absence of disc spines in *Ophiarthrum*. However, this could be considered the end point of a severe reduction in the density of disc spines shown in other *Ophiomastix* species (*flaccida*, *venosa*, *variabilis*). The species *pictum*, *elegans* and *flaccida* shared some important autapomorphies such as the absence of a calcareous septum that separates the radial nerve and water canal on the basal arm vertebra, and the considerable rearrangement of the mitochondrial genome, and may deserve recognition as a subgenus.The genus-level synonymy resulted in the name *Ophiomastix elegans* Brock, 1888 being a homonym of *Ophiomastix* (formerly *Ophiarthrum*) *elegans* (Peters, 1851). Consequently, we propose the replacement name: *Ophiomastix brocki* O'Hara (urn:lsid:zoobank.org:act:C759B2F8-FE07-41E3-8E2A-C4029C5E148C in publication: urn:lsid:zoobank.org:pub:5D77CC09-641C-437F-9357-B87C06C31C0) for the former species. Two of the other included species had characters typical of many other *Ophiomastix* species: 'Ophiocoma' *endeani* had the elongated granules on the ventral disc surface (Endean 1963), swollen tips of some arm spines (Endean 1963), and a large lecithotrophic egg (approx. 340 μm, Table 1) and 'Ophiocoma' *wendtii* possessed long claviform upper arm spines (Hendler et al. 1995). Our morphological analysis (see below) provided evidence that three additional species *Ophiomastix marshallensis*, *O. ornata* and *O. corallicola*, for which we have no genetic data, should be provisionally retained in the genus *Ophiomastix*.

The remaining scolopendrina-group species formed a monophyletic clade for which we retain the name *Ophiocoma* (in a restricted sense) as it included the type species *O. echinata*. The species *O. anaglyptica* was morphologically divergent (flattened plate-like disc granules ventrally, a few short disc spines, flask-shaped upper arm spines). For this species we obtained only a short (384 bp) sequence of the mitochondrial 16S gene from an old (1985)

museum specimen and additional genetic data is desirable to confirm its inclusion within *Ophiocoma*. The pumila-group of *Ophiocoma* (*alexandri*, *pumila*, *valenciae*) were paraphyletic with respect to the three nominal *Ophiocomella* species, and we consider all six species to form an expanded *Ophiocomella*. Finally the pica-group of *Ophiocoma* species were paraphyletic with respect to the brevipes-group (named as the subgenus *Breviturma* by Stöhr et al. 2013, and raised to genus by O'Hara et al. 2018). Consequently we consider both groups to belong to a single genus *Breviturma*.

In several cases, multiple samples from the same nominal species were quite genetically divergent indicating the possible presence of cryptic or allopatric species, such as between Easter Is (*Breviturma longispina*1) and French Polynesian (*B. longispina*2) samples, and between western Indian Ocean (*Ophiocoma* cf *erinaceus* and *Breviturma* cf *dentata*) and western Pacific Ocean samples (*O. erinaceus* and *B. dentata*). Conversely, the species limits within the *Ophiomastix brocki/macroplaca* and the fissiparous *Ophiocomella* clade were unclear and require further study. The *Ophiocoma* sample found on Clipperton Island ("erinaceus2") belonged to the Indo-Pacific *O. erinaceus* complex, rather than one of the species found on the American Pacific coast.

3.3. Morphological and life history characters

We collated states or mean values for 36 adult morphological characters, used previously in taxonomic diagnoses, across 43 taxa. The resulting matrix was 93% data complete (Table S2). A PCoA ordination (Fig. 6a) separated *Ophiocomella* and *Breviturma* from a combined *Ophiomastix*/*Ophiocoma*. However, there was multivariate dispersion in *Ophiocomella, Breviturma* and *Ophiomastix*: within *Ophiocomella*, the fissiparous and non-fissiparous species of Ophiocomella separated, within *Breviturma*, the "brevipes' and 'pica' groups (*sensu* Devaney 1970) separated, and within *Ophiomastix*, the species with tall disc spines or naked discs, separated from those species with disc granules and/or short spines. The later overlapped with the 'scolopendrina' group of *Ophiocoma*, which both share alternating arm spines. The ordination emphasised the pleisiomorphic nature of many traditional taxonomic characters.

The relative MDI (within clade mean morphological Euclidian distance) (Fig. 6b, Table S4) was notably high in the *Ophiomastix* radiation (up to 0.72), a result confirming the wide

scatter of *Ophiomastix* species across the PCoA plot. High MDI also occurred at the node subtending the fissiparous clade of *Ophiocomella* (0.80) and nodes separating the major genera.

To explore the life history of the group, 13 species were spawned and cultured for this study. Additional data were obtained from museum specimens (10 species) or from the literature (3 species) (Table 1). The vast majority of the species had small eggs (<=100 μm) and (at least putatively) planktotrophic development. Species with large green buoyant eggs (>340 μm), and lecithotrophic development, were restricted to *Ophiomastix*. Another three *Ophiomastix* species were found from museum specimens to have immature eggs that exceeded 200 μm and were putatively lecithotrophic. However, whether these lecithotrophs formed a monophyletic clade was uncertain. Our phylogenetic reconstructions could not unequivocally resolve the basal topology of *Ophiomastix* (Fig. 2), leaving species with planktotrophic development (e.g. *O. wendtii*, *O. occidentalis*) in a polytomy with the lecithotrophs. Crucially the phylogenetic position of *O. variabilis* and *O. palaoensis* was uncertain (77/0.89 BS/LPP support) and their development unknown. The genus *Ophiomastix* displayed morphological variability, however, the topological uncertainty prevented us from determining whether the transition to lecithotrophy preceded or accompanied an adaptive radiation in morphospace. Nevertheless, the lecithotrophic species exhibit a variety of morphologies not seen elsewhere in the ophiocomids, including variable arm length, tall sparse disc spines, and colour patterns (notably with reds and yellows).

Asexual reproduction (fissiparity) was limited to one species complex (*ophiactoides-schmitti-sexradia*) within *Ophiocomella*, which corresponded to a limited change in morphospace (Fig. 6). The presence of an ornate egg was limited to the *Ophiocoma* clade (as restricted herein).

4. Discussion

The high power afforded by phylogenomic-scale data of 1465 exons in 416 genes allows us to incorporate both concatenated data and individual gene-tree inference into the interpretation of phylogenetic tempo and pattern, in particular to distinguish and demark unequivocal clades that are appropriate for taxonomic, evolutionary and biogeographic discussion. Genomic-scale multi-locus data also provides a rich source of evidence for

discovering and investigating unusual and unexpected genomic and demographic phenomena, and we describe several examples below.

Our phylogenetic topology was largely consistent between concatenated data and gene-tree approaches and (with a few exceptions) most nodes had high statistical support. Several parts of the phylogeny are characterised by short internodes indicative of rapid (within the anomalous zone) or non-hierarchical cladogenesis (Linkem et al. 2016). This occurred near the crown of the *Ophiomastix* clade as well as in more recent radiations within species complexes (e.g. *Ophiocoma schoenleini-cynthiae*, and *Breviturma brevipes-doederleini*) leading to some minor topological variation and lowered node support. Some additional local topological instability was induced by the incorporation of three species (*Ophiocoma anaglyptica*, *Ophiocomella schmitti*, *Ophiomastix macroplaca*) with only mtDNA using a super-matrix approach, although their generic placement was in accordance with their morphological characters and traditional taxonomic position. We confirmed the generic placement of a further three species (*Ophiomastix corallicola*, *O. marshallensis*, and *O. ornata*), for which we had no genetic data, by ordinating morphological data.

The StarBEAST2 multi-species coalescent analysis broadly re-iterated the results of the concatenated BEAST and ASTRAL species-tree analyses, including clade age (with exceptions, see below). All analyses had equivocal support at the base of the *Ophiomastix* and *Breviturma* radiations, which were also characterised by short internodes, within some of the younger species complexes.

The mitochondrial genes of *Ophiomastix flaccida* and *O. pictum* appeared very divergent, and significantly more GT rich than other ophiocomids. Both direct PCR and genomic read data were consistent in identifying these sequences as true mitochondrial genes and not contaminants or paralogs. We suspected that their distinctiveness was, at least in part, a result of a substantial mitogenomic reorganisation in the clade. While our assessment of mitogenome gene order was provisional, the data were consistent with the idea that several genes, including COI and 16S have changed coding strands relative to other taxa. Due to asymmetric replication, the two mtDNA strands typically have different base compositions (the so called heavy and light strands, Bernt et al. 2013a). Hence, a change in strand coding can drive base compositional change, resulting in high apparent sequence divergence. Mitogenomic rearrangement, and subsequent compensatory changes, likely further

accelerates divergence (Bernt et al. 2013a). The marked increase (three-fold) in the level of divergence in nuclear encoded mitochondrial functioning proteins (N-mt) versus general cytosolic proteins in *flaccida* and *pictum* is consistent with the hypothesis of correlated evolution between co-functioning nuclear and mitochondrial encoded proteins (Havird et al. 2015). Whatever the process, both the mtDNA and N-mt genes of *flaccida* and *pictum* mtDNA were very divergent, consistent with major genomic upheaval in their mitochondrial evolution (Havird et al. 2015) and worthy of further study.

Multi-locus phylogenomic data also allowed us an (albeit preliminary) investigation of the genomic architecture of the 6-armed *Ophiocomella* species. Populations in the Caribbean (*O. ophiactoides*) have been found to reproduce both asexually (through fissiparity) and sexually. The gonads were functional (although with low fecundity) giving rise to pelagic feeding larvae (Mladenov and Emson 1984). However, many individuals in these studies showed evidence of having regrown from binary fission (Mladenov et al. 1983) and allozyme data suggested clonal reproduction was much more frequent than larval settlement (Mladenov and Emson 1990). We found relatively high levels of within sample polymorphism in this group, possibly indicating a 1) very large effective population size, 2) hybrid origins (diploid from slightly diverged lineages), or 3) allelic divergence following the onset of asexual reproduction (the 'Meselson effect', Birky 1996). While the low mitochondrial diversity and probable excess heterozygosity argue against large effective population size, properly assessing the three options will require full analysis of allele and genotype patterns in population samples (Ament-Velasquez et al. 2016). Rather than separate species, *ophiactoides* and *sexradia* (and probably *schmitti*) may be better thought of as samples from a larger facultative asexual complex (Birky and Barraclough 2009). Wide range/recent dispersal is a feature of such complexes (Tilquin and Kokko 2016), consistent with the extraordinary distribution of fissiparous *Ophiocomella*.

4.1. Taxonomy

The pre-existing genus-level taxonomy was inadequate. Notably the type genus *Ophiocoma* was polyphyletic (Fig. 2) and required taxonomic revision. Our phylogenetic reconstruction recovered four major clades, each separated by relatively long stem to crown ages, with unequivocal support from both concatenated gene bootstrap support and multi-locus coalescent gene-tree congruence. We recognised these four clades as genera and

assigned them available generic names. They were broadly interpretable in terms of informal species-groups identified by traditional taxonomy (Devaney 1970). The four groups were: 1) *Ophiomastix*, which was expanded to contain species formerly in *Ophiarthrum* and four species from the scolopendrina-group of *Ophiocoma*; 2) *Ophiocoma*, restricted to the remaining scolopendrina-group species; 3) *Ophiocomella*, which included the fissiparous *Ophiocomella* species and the pumila-group of *Ophiocoma*; and 4) *Breviturma*, which included the pica- and brevipes-groups of *Ophiocoma* (Fig. 2 and 3, see results for more details). Taxonomic consequences of this genus-level revision were that the genus *Ophiarthrum* became a synonym of *Ophiomastix* and the new replacement name *Ophiomastix brocki* was proposed for *Ophiomastix elegans* Brock, 1888, as it became a homonym of *Ophiomastix* (formerly *Ophiarthrum*) *elegans* (Peters, 1854).

The crown-age of the four identified genera varied from ~30 (*Ophiocomella*) to ~60 my (*Breviturma*), far older than that proposed for vertebrate genera (2-5 my, Avise and Johns 1999). However, applying the latter scheme to the ophiocomids would result in every species complex becoming a genus and involve considerable disruption to existing taxonomy. Moreover, we considered that the lack of resolution across basal nodes of *Ophiomastix* and *Breviturma* precluded further subdivision.

4.2. Developmental and morphological transitions

Lecithotrophy appeared to have a single origin in ophicomids, although our current phylogenetic resolution and life history data were insufficient to demonstrate this with certainty (Fig. 6B). Species with lecithotrophic development, previously dispersed among *Ophiomastix*, *Ophiarthrum*, and *Ophiocoma*, fell into a single clade within the redefined genus *Ophiomastix.* Developmental transition from planktotrophy to lecithotrophy has occurred infrequently in echinoderms. For example, the transition has occurred only seven times across the extant Echinoidea (Wray 1996). *Ophiomastix* exhibits the greatest adult morphological diversity among ophiocomid genera (Fig. 6). The development of lecithotrophy appears to be yet another expression of phenotypic variability in the genus.

Possession of an ornate (thorny) egg fertilisation envelope was limited to the genus *Ophiocoma* (as restricted here), and has not been reported for any other ophiuroid group (Cisternas et al. 2013). As suggested for chiton species that also have an ornate fertilisation

envelope, this elaboration may have evolved to either guide sperm to specific entry sites or to improve the buoyancy/dispersal of the progeny (Cisternas et al. 2013). This character does not appear to have been accompanied by a sudden transition in adult morphology: the *Ophiocoma* crown node has a low relative MDI (0.10) and occupied relatively limited morpho-space (Fig. 6).

Fissiparous (splitting into two halves) asexual development appears to have a single origin, confined to one clade within *Ophiocomella*. This clade differed most obviously from cogeners in having six arms, the presence of a water ring pore within the adradial muscle scar of the oral plate, and adoral shields that meet proximal to the oral shields, resulting in a relatively high MDI (0.29, Fig. 6b) and separation of the two groups on the PCoA plot (Fig. 6a). The presence of six or more arms has been often associated with fissiparity across the Ophiuroidea and Asteroidea (Emson and Wilkie 1980). The water ring pore may also be a consequence of a fissiparous habit as it also has been reported from the fissiparous *Ophiactis savignyi* (Devaney 1970). Despite these differences, fissiparous and non-fissiparous species of *Ophiocomella* shared many other characters (e.g. shape of arm and disc spines) and the Caribbean species *O. pumila* and *O. ophiactoides* have often been confused with each other (Parslow and Clark 1963, Mladenov and Emson 1984).

Another shift in morphology, not related to a known life history change, was inferred to have occurred along the long stem of the brevipes-dentata lineage of *Breviturma* as indicated from the MDI results (0.32, Fig. 6b) and PCoA plots (Fig. 6a). This included a short area of tooth papillae on the dental plate and a complete dense coat of small granules over the disk, the former character possibly related to their deposit feeding habitat (Chartock 1983).

A surprising outcome of our new phylogeny was the lack of monophyly between species with alternating numbers of arm spines on successive segments. For example, in *Ophiocoma erinaceus*, there are three arm spines on one side of the arm segment and four on the other, with the reverse occurring on the next segment. This alternating pattern occurs on all species in the revised *Ophiocoma* and *Ophiomastix*. However, our phylogeny does not have *Ophiocoma* as sister to *Ophiomastix,* as predicted by Devaney (1978), but to *Ophiocomella* which has non-alternating arm spines.

In summary, morphological evolution within the Ophiocomidae has been mostly gradual since its origin ~90-110 my. Few characters have arisen that can be used to uniquely identify taxa above species level. Although morphological stasis is a problem for the taxonomist, it is clearly not a problem for ophiocomids which dominate the ophiuroid fauna of coral reefs worldwide.

4.3. Biogeography

The removal of the genera *Ophiopsila*, *Clarkcoma*, *Ophiopteris* and *Ophiocomina* has resulted in the Ophiocomidae being (almost exclusively) a circumtropical (<30° latitude), shallow water (<100 m) taxon (O'Hara et al. 2017). Only a few species extended to 35°N (e.g. Bermuda) or 35°S (Australia, South Africa) or into deeper water (outer shelf or upper bathyal depths), notably the *Ophiomastix brocki*-*O. macroplaca* complex and *O. palaoensis*.

The evolutionary dynamics of ophiocomids parallels the Cenozoic diversification of their modern coral reef habitats (Veron 1995). The diversification of the four genera proposed here was ancient, their crown ages dating from 30 to 60 my. This predates the gradual closure of the pan-tropical Tethys Seaway that occurred from the Oligocene (34 my) to middle Miocene (11-13 my), separating the Atlantic/East Pacific and Indo-West Pacific faunas (Harzhauser et al. 2007, Cowman and Bellwood 2013). All four genera have representatives in both the Atlantic and the Indo-Pacific, with node ages that considerably predate the final closure, including 50.0 ± 13 my (subtending *Breviturma paucigranulata*), 49.6 ± 12 my (*Ophiomastix wendtii*), 33.7 ± 11 my (*Ophiocoma erinaceus/aethiops*) and 29.3 ± 10 my (*Ophiocomella valenciae/alexandri*). Similarly, species pairs putatively generated by the formation of the Isthmus of Panama, were here dated to 11.7 ± 6 my (*Ophiocoma echinata*/*aethiops*) and 14.1 ± 6 my (*Ophiocomella pumila*/*alexandri*), again considerably predating the final closure (2.8 my, Lessios 2008). Although, these vicariant events have been used as a calibration point in many phylogenies, clearly they did not represent short-lived episodes in geological time, but involved processes of pre-closure biotic regionalisation, intermittent seaway closure, and post-closure extinction events, occurring over millions of years (Lessios 2008, Montes et al. 2012, Bacon et al. 2015).

One species has managed to transverse the East Pacific Barrier (Lessios et al. 1998, Cowman and Bellwood 2013). We confirmed here that the *Ophiocoma* species found on

669 Clipperton Island, 1,080 km SW of Mexico and 3,200 km NE of the Marquesas Islands, was
670 the Indo-Pacific *Ophiocoma erinaceus* (see Devaney 1974) not *O. scolopendrina* as
671 originally reported by A.H Clark (1939).
672
673 Relationships between West Indian Ocean and central Indo-West Pacific clades fell into
674 two categories. There are three relatively old West Indian Ocean endemic lineages, dated to
675 18.7 ± 5 (*Ophiomastix venosa*), 20.8 ± 8 (*Ophiocomella valenciae*) and 22.8 ± 6
676 (*Ophiomastix koehleri*). A second group of species (or species complexes) appear to be
677 distributed across the Indian Ocean, including *Breviturma brevipes*, *B. dentata*, *B.*
678 *doederleini*, *B. krohi, B. pica*, *B. pusilla*, *Ophiocoma cynthiae*, *O. erinaceus*, *O. schoenleini*,
679 *O. scolopendrina*, *Ophiomastix elegans*, *O. pictum*, and *O. variabilis*. Molecular data
680 indicates that there is sufficient genetic distance between western and eastern clades to
681 suggest allopatric speciation within *O. erinaceus*, *B. dentata*, *B. brevipes*, *B. doederleini*, *B.*
682 *pica* and *B. pusilla* (Hoareau et al. 2013, Boissin et al. 2017, this work). Conversely, *O.*
683 *cynthiae*, *B. krohi*, *O. scolopendrina* cannot be divided into eastern and western lineages
684 (Hoareau et al. 2013), suggesting that there has been recent gene flow across the Indian
685 Ocean. A characteristic of this family is that many Indo-Pacific species occur in sympatry, for
686 example 18 species have been recorded from shallow water (0-20 m) around Lizard Island on
687 the Great Barrier Reef, although they can occupy subtly different microhabitats (Byrne and
688 O'Hara 2017).
689
690 The fissiparous *Ophiocomella* clade has been exceptional in achieving a relatively rapid
691 worldwide equatorial distribution. We found the three fissiparous species (*sexradia*, *schmitti*
692 and *ophiactoides*, allopatrically distributed in the Indo-West Pacific, eastern Pacific and
693 western Atlantic respectively) to be genetically very similar (although with high allelic
694 diversity, see above) and possibly represent a single species-complex. This complex can
695 potentially disperse via pelagic feeding larvae or by adults rafting on seaweed, sponges or
696 even human shipping, as has been suggested for other small shallow water fissiparous
697 ophiuroids (Hendler et al. 1999a, Roy and Sponer 2002). The successful establishment of
698 new colonies is improved through requiring only one colonist and the potential to rapidly
699 expand populations through asexual reproduction (Tilquin and Kokko 2016).
700

Appendix A. Supplementary material

S1. List of samples
S2. Ophiocomid adult character matrix
S3. PCoA species scores for 5 axes
S4. Mitogenome gene order information
S5. RAxML analysis of nuclear exon data.
S6. ASTRAL-II species tree of nuclear exon data.
S7. RAxML analysis of the exon+mtDNA super-matrix.
S8. StarBEAST analysis of nuclear exon data.
S9. Morphological Disparity Index results.

Author contributions

TOH, PC and MB conceived the study; PC obtained the larval/developmental data and 16S sequences; TOH measured the morphological data; TOH, GBC, JS, GP, PC, and MB obtained the tissue samples and contributed distributional data; AH compiled the phylogenomic datasets; AH and GBC conducted all the phylogenetic and morphometric analyses; TOH and AH took the lead in, and other authors contributed to, writing the manuscript.

Acknowledgements

TOH and AFH were supported by the Marine Biodiversity Hub, funded through the National Environmental Research Program (NERP), and administered through the Australian Government's Department of the Environment. MB was supported by the Australian Research Council (DP034413). MB, TOH and PC were also supported by a grant from the Raine Island Corporation. The authors thank the many museum curators, collection managers and researchers who facilitated the tissue sampling, most notably Marc Eléaume (MNHN), Tania Pineda-Enriquez (FMNH), Francisco Solis-Marin (UNAM), Cynthia Ahearn (USNM, deceased), Erin Easton (Universidad Católica del Norte, Chile), and Scott Godwin (BPBM). We also thank Sumitha Hunjan and Kate Naughton (MV) for extracting DNA and assembling plates for exon-capture, and Declan O'Hara for the layout of Fig. 1.

735 **References**
736
737 Altschul S.F., Madden T.L., Schäffer A.A., Zhang J., Zhang Z., Miller W., Lipman D.J. 1997.
738 Gapped BLAST and PSI-BLAST: a new generation of protein database search programs.
739 Nucleic Acids Res. 25,3389-3402.
740 Ament-Velasquez S.L., Figuet E., Ballenghien M., Zattara E.E., Norenburg J.L., Fernández-
741 Álvarez F.A., Bierne J., Bierne N., Galtier N. 2016. Population genomics of sexual and
742 asexual lineages in fissiparous ribbon worms (*Lineus*, Nemertea): hybridization,
743 polyploidy, and Meselson effect. Mol. Ecol. 25,3356–3369.
744 Avise J.C., Johns G.C. 1999. Proposal for a standardized temporal scheme of biological
745 classification for extant species. Proc. Natl. Acad. Sci. 96,7358-7363.
746 Bacon C.D., Silvestro D., Jaramillo C., Smith B.T., Chakrabarty P., Antonelli A. 2015.
747 Biological evidence supports an early and complex emergence of the Isthmus of Panama.
748 Proc. Natl. Acad. Sci. USA 112,6110-6115.
749 Balloux F., Lehmann L., de Meeus T. 2003. The population genetics of clonal and partially
750 clonal diploids. Genetics 164, 1635–1644.
751 Bernt M., Braband A., Schierwater B., Stadler P.F. 2013a. Genetic aspects of mitochondrial
752 genome evolution. Mol. Phylogenet. Evol. 69,328-338.
753 Bernt M., Donath A., Jühling F., Externbrink F., Florentz C., Fritzsch G., Pütz J., Middendorf
754 M., Stadler P.F. 2013b. MITOS: Improved de novo Metazoan Mitochondrial Genome
755 Annotation. Mol. Phylogenet. Evol. 69,313-319.
756 Birky C.W. 1996. Heterozygosity, Heteromorphy, and Phylogenetic Trees in Asexual
757 Eukaryotes. Genetics 144,427–437.
758 Birky C.W., Barraclough T.G. 2009. Asexual speciation. In: Schön I, Martens K, van Dijk P
759 editors. Lost Sex. Amsterdam, The Netherlands, Springer, p. 201–216.
760 Boissin E., Hoareau T.B., Bruggemann J.H., Paulay G. 2017. DNA barcoding of reef brittle-
761 stars from the South western Indian Ocean evolutionary hotspot. Ecol. Evol. 7,11197-
762 11203.
763 Bouckaert R., Heled J., Kühnert D., Vaughan T., Wu C.-H., Xie D., Suchard M.A., Rambaut
764 A., Drummond A.J. 2014. BEAST 2: A Software Platform for Bayesian Evolutionary
765 Analysis. PLoS Comput. Biol. 10,e1003537.
766 Bouckaert R.R. 2010. DensiTree: Making sense of sets of phylogenetic trees. Bioinformatics
767 26,1372–1373.

768 Brock J. 1888. Die Ophiuridenfauna des indischen Archipels. Zeitschrift für
769 Wissenschaftliche Zoologie 47,465-539.
770 Byrne M., O'Hara T.D. 2017. Australian Echinoderms: Biology, ecology and evolution.
771 Melbourne and Canberra, CSIRO Publishing and ABRS p. 612.
772 Chartock M.A. 1983. Habitat and feeding observations on species of *Ophiocoma*
773 (Ophiocomidae) at Enewetak. Micronesica 19,131-149.
774 Cisternas P., O'Hara T.D., Byrne M. 2013. An ornate fertilisation envelope is characteristic of
775 some *Ophiocoma* species (Ophiuroidea: Ophiocomidae). In: Johnson C editor.
776 Echinoderms in a Changing World. Proceedings of the 13th International Echinoderm
777 Conference, University of Tasmania, Hobart Tasmania, Australia, 5-9 January 2009.
778 London, Taylor & Francis, p. 229-231.
779 Cisternas P., Selvakumaraswamy P., Byrne M. 2004. Evolution of development and the
780 Ophiuroidea-revisited. In: Heinzeller T, Nebelsick J editors. Echinoderms: München:
781 Proceedings of the 11th International Echinoderm Conference, Munich, Germany, 6-10
782 October 2003. Leiden, Balkema, p. 521-526.
783 Clark A.H. 1939. Echinoderms (other than holothurians) collected on the Presidential Cruise
784 of 1938. Smithson. misc. collect. 98,1–18 pls 11–15.
785 Cowman P.F., Bellwood D.R. 2013. Vicariance across major marine biogeographic barriers:
786 temporal concordance and the relative intensity of hard versus soft barriers. Proc. Roy.
787 Soc. B 280,20131541.
788 de Queiroz A., Gatesy J. 2007. The supermatrix approach to systematics. Trends Ecol. Evol.
789 22,34-41.
790 Degnan J.H., Rosenberg N.A. 2009. Gene tree discordance, phylogenetic inference and the
791 multispecies coalescent. Trends Ecol. Evol. 24,332–340.
792 Delroisse J., Fourgon D., Eeckhaut I. 2013. Reproductive cycles and recruitment in
793 *Ophiomastix venosa* and *Ophiocoma scolopendrina*, two co-existing tropical ophiuroids
794 from the barrier reef of Toliara (Madagascar). Cah. Biol. Mar. 54,593-603.
795 Devaney D.M. 1968. The systematics and post-larval growth changes in ophiocomid
796 brittlestars. Zoology, University of Hawaii, p. 292.
797 Devaney D.M. 1970. Studies on ophiocomid brittlestars. 1. A new genus (*Clarkcoma*) of
798 Ophiocominae with a reevaluation of the genus *Ophiocoma*. Smithson. Contr. Zool. 51,1-
799 41.
800 Devaney D.M. 1974. Shallow-water asterozoans of south-eastern Polynesia. 2. Ophiuroidea.
801 Micronesica 10,105-204.

802 Devaney D.M. 1978. A review of the genus *Ophiomastix* (Ophiuroidea: Ophiocomidae).
803 Micronesica 14,273-359.
804 Emson R.H., Wilkie I.C. 1980. Fission and autotomy in echinoderms. Oceanogr. Mar. Biol.
805 Annu. Rev. 18,155-250.
806 Endean R. 1963. A new species of brittle-star (Echinodermata: Ophiuridea) from northern
807 New South Wales. Proc. Linn. Soc. N.S.W. 88,295-297 fig. 291 pl. 217.
808 Fourgon D., Eeckhaut I., Vaïtilingon D., Jangoux M. 2005. Lecithotrophic development and
809 metamorphosis in the Indo-West Pacific brittle star *Ophiomastix venosa* (Echinodermata:
810 Ophiuroidea). Invertebr. Reprod. Dev. 47,155-165.
811 Fourgon D., Jangoux M., Eeckhaut I. 2007. Biology of a "babysitting" symbiosis in brittle
812 stars: analysis of the interactions between *Ophiomastix venosa* and *Ophiocoma*
813 *scolopendrina*. Invertebr. Biol. 126,385-395.
814 Grabherr M.G., Haas B.J., Yassour M., Levin J.Z., Thompson D.A., Amit I., Adiconis X.,
815 Fan L., Raychowdhury R., Zeng Q., Chen Z., Mauceli E., Hacohen N., Gnirke A., Rhind
816 N., di Palma F., Birren B.W., Nusbaum C., Lindblad-Toh K., Friedman N.*, et al.* 2011.
817 Full-length transcriptome assembly from RNA-Seq data without a reference genome. Nat.
818 Biotechnol. 29,644–652.
819 Harmon L.J., Schulte J.A., Larson A., Losos J.B. 2003. Tempo and Mode of Evolutionary
820 Radiation in Iguanian Lizards. Science 301,961-964.
821 Harmon L.J., Weir J.T., Brock C.D., Glor R.E., Challenger W. 2008. GEIGER: investigating
822 evolutionary radiations. Bioinformatics 24,129-131.
823 Harzhauser M., Kroh A., Mandic O., Piller W.E., Göhlich U., Reuter M., Berning B. 2007.
824 Biogeographic responses to geodynamics: A key study all around the Oligo–Miocene
825 Tethyan Seaway. Zool. Anz. 246,241-256.
826 Havird J.C., Whitehill N.S., Snow C.D., Sloan D.B. 2015. Conservative and compensatory
827 evolution in oxidative phosphorylation complexes of angiosperms with highly divergent
828 rates of mitochondrial genome evolution. Evolution 69,3069–3081.
829 Hendler G. 1984. Brittlestar colour-change and phototaxis (Echinodermata: Ophiuroidea:
830 Ophiocomidae). Mar. Ecol. 5,379-401.
831 Hendler G., Baldwin C.C., Smith D.G., Thacker C.E. 1999a. Planktonic dispersal of juvenile
832 brittle stars (Echinodermata: Ophiuroidea) on a Caribbean Reef. Bull. Mar. Sci. 65,283-
833 288.

834 Hendler G., Grygier M.J., Maldonado E., Denton J. 1999b. Babysitting brittle stars:
835 heterospecific symbiosis between ophiuroids (Echinodermata). Invertebr. Biol. 118,190-
836 201.
837 Hendler G., Miller J.E., Pawson D.L., Kier P.M. 1995. Sea stars, sea urchins and allies:
838 Echinoderms of Florida and the Caribbean. Smithsonian Institution Press Washington.
839 Hoareau T.B., Boissin E., Paulay G., Bruggemann J.H. 2013. The Southwestern Indian Ocean
840 as a potential marine evolutionary hotspot: perspectives from comparative phylogeography
841 of reef brittle-stars. J. Biogeogr. 40,2167–2179.
842 Hugall A.F., O'Hara T.D., Hunjan S., Nilsen R., Moussalli A. 2016. An exon-capture system
843 for the entire class Ophiuroidea. Mol. Biol. Evol. 33,281–294.
844 Lanier H.C., Knowles L.L. 2012. Is recombination a problem for species-tree analyses? Syst.
845 Biol. 61,691–701.
846 Lessios H.A. 2008. The great American schism: divergence of marine organisms after the rise
847 of the central American isthmus. Annu. Rev. Ecol. Evol. Syst. 39,63-91.
848 Lessios H.A., Kessing B.D., Robertson D.R. 1998. Massive gene flow across the world's
849 most potent marine barrier. Proc. Roy. Soc. B 265,583-588.
850 Linkem C.W., Minin V.N., Leaché A.D. 2016. Detecting the Anomaly Zone in Species Trees
851 and Evidence for a Misleading Signal in Higher-Level Skink Phylogeny (Squamata:
852 Scincidae). Syst. Biol. 65,465-477.
853 Maechler M., Rousseeuw P., Struyf A., Hubert M., Hornik K. 2017. cluster: Cluster Analysis
854 Basics and Extensions. R package version 2.0.6.
855 Martynov A.V. 2010. Reassessment of the classification of the Ophiuroidea (Echinodermata),
856 based on morphological characters. I. General character evaluation and delineation of the
857 families Ophiomyxidae and Ophiacanthidae. Zootaxa 2697,1-154.
858 Matsumoto H. 1915. A new classification of the Ophiuroidea: with descriptions of new
859 genera and species. Proc. Acad. Nat. Sci. Phil. 67,43-92.
860 McEdward L.R., Miner B.G. 2001. Larval and life-cycle patterns in echinoderms. Can. J.
861 Zool. 79,1125-1170.
862 Mirarab S., Reaz R., Bayzid M.S., Zimmermann T., Swenson M.S., Warnow T. 2014.
863 ASTRAL, genome-scale coalescent-based species tree estimation. Bioinformatics
864 30,i541–i548.
865 Mirarab S., Warnow T. 2015. ASTRAL-II: coalescent-based species tree estimation with
866 many hundreds of taxa and thousands of genes. Bioinformatics 31,i44–i52.

867 Mladenov P.V. 1985. Development and metamorphosis of the brittle star *Ophiocoma pumila*:
868 evolutionary and Ecological implications. Biol. Bull. 168,285-295.
869 Mladenov P.V., Emson R.H. 1984. Divide and broadcast: sexual reproduction in the West
870 Indian brittle star *Ophiocomella ophiactoides* and its relationship to fissiparity. Mar. Biol.
871 81,273-282.
872 Mladenov P.V., Emson R.H. 1990. Genetic structure of populations of two closely related
873 brittle stars with contrasting sexual and asexual life histories, with observations on the
874 genetic structure of a second asexual species. Mar. Biol. 104,265-274.
875 Mladenov P.V., Emson R.H., Colpitts L.V., Wilkie I.C. 1983. Asexual reproduction in the
876 West Indian brittle star *Ophiocomella ophiactoides* (H. L. Clark) (Echinodermata:
877 Ophiuroidea). J. Exp. Mar. Bio. Ecol. 72,1-23.
878 Montes C., Cardona A., McFadden R., Morón S.E., Silva C.A., Restrepo-Moreno S., Ramírez
879 D.A., Hoyos N., Wilson J., Farris D., Bayona G.A., Jaramillo C.A., Valencia V., Bryan J.,
880 J.A. F. 2012. Evidence for middle Eocene and younger land emergence in central Panama:
881 Implications for Isthmus closure. GSA Bulletin 124,780-799.
882 Mortensen T. 1921. Studies of the study of the development and larval forms of echinoderms.
883 G.E.C Gad Copenhagen.
884 Mortensen T. 1937. Contributions to the study of the development and larval forms of
885 echinoderms. IV. Kgl. dan. vidensk. selsk. skr. naturvidensk. math afd. 7,1-65.
886 Nguyen L.-T., Schmidt H.A., von Haeseler A., Minh B.Q. 2015. IQ-TREE: A fast and
887 effective stochastic algorithm for estimating maximum likelihood phylogenies. Mol. Biol.
888 Evol. 32,268-274.
889 O'Hara T.D., Byrne M., Cisternas P. 2004. The *Ophiocoma erinaceus* complex: another case
890 of cryptic speciation in echinoderms. In: Heinzeller T, Nebelsick JH editors. Echinoderms:
891 München: Proceedings of the 11th International Echinoderm Conference, Munich,
892 Germany, 6-10 October 2003. Leiden, Balkema, p. 537-542.
893 O'Hara T.D., Hugall A.F., Thuy B., Moussalli A. 2014. Phylogenomic resolution of the Class
894 Ophiuroidea unlocks a global microfossil record. Curr. Biol. 24,1874-1879.
895 O'Hara T.D., Hugall A.F., Thuy B., Stöhr S., Martynov A.V. 2017. Restructuring higher
896 taxonomy using broad-scale phylogenomics: the living Ophiuroidea. Mol. Phylogenet.
897 Evol. 107,415-430.
898 O'Hara T.D., Stöhr S., Hugall A.F., Thuy B., Martynov A.V. 2018. Morphological diagnoses
899 of higher taxa in Ophiuroidea (Echinodermata) in support of a new classification. Eur. J.
900 Taxon. 416,1–35.

Oak T., Scheibling R.E. 2006. Tidal activity and feeding behaviour of the ophiuroid *Ophiocoma scolopendrina* on a Kenyan reef flat. Coral Reefs 25,213-222.

Ogilvie H.A., Bouckaert R.R., Drummond A.J. 2017. StarBEAST2 Brings Faster Species Tree Inference and Accurate Estimates of Substitution Rates. Mol. Biol. Evol. 34,2101-2114.

Olbers J.M., Samyn Y. 2012. The *Ophiocoma* species (Ophiurida: Ophiocomidae) of South Africa. Western Indian Ocean J. Mar. Sci. 10,137-154.

Palumbi S.R., Martin A., Romano S., McMillan W.O., Stice L., Grabowiski G. 1991. The simple fools guide to PCR. Ver 2.0. University of Hawaii Honolulu.

Paradis E., Claude J., Strimmer K. 2004. APE: analyses of phylogenetics and evolution in R language. Bioinformatics 20.

Parslow R.E., Clark A.M. 1963. Ophiuroids of the Lesser Antilles. Studies on the Fauna of Curaçao and other Caribbean Islands 15,24-50.

Peters W.C.H. 1851. Übersicht der von ihm an der Küste von Mossambique eingesammelten Ophiuren, unter denen sich zwei neue Gattungen befinden. Ber. K. Preuss. Akad. Wiss. Berl. 1851,463-466.

Roy M.S., Sponer R. 2002. Evidence of a human-mediated invasion of the tropical western Atlantic by the 'world's most common brittlestar'. Proc. Roy. Soc. B 269,1017-1023.

Sayyari E., Mirarab S. 2016. Fast coalescent-based computation of local branch support from quartet frequencies. Mol. Biol. Evol.,doi: 10.1093/molbev/msw1079.

Selvakumaraswamy P., Byrne M. 2000. Reproduction, spawning, and development of five ophiuroids from Australia and New Zealand. Invertebr. Biol. 119,394-402.

Sewell M.A., Young C.M. 1997. Are echinoderm egg size distributions bimodal? Biol. Bull. 193,297-305.

Stamatakis A. 2014. RAxML Version 8: A tool for Phylogenetic Analysis and Post-Analysis of Large Phylogenies. Bioinformatics 30,1312-1313.

Strathmann M.F. 1987. Reproduction and development of marine invertebrates of the northern Pacific coast: data and methods for the study of eggs, embryos and larvae. University of Washington Press Seattle.

Sumner-Rooney L., Rahman I.A., Sigwart J.D., Ullrich-Lüter E. 2018. Wholebody photoreceptor networks are independent of ‘lenses’ in brittle stars. Proc. Roy. Soc. B 285,20172590.

933 Thuy B., Stöhr S. 2016. A New Morphological Phylogeny of the Ophiuroidea
934 (Echinodermata) Accords with Molecular Evidence and Renders Microfossils Accessible
935 for Cladistics. PLosONE 11,e0156140.
936 Tilquin A., Kokko H. 2016. What does the geography of parthenogenesis teach us about sex?
937 Philos. Trans. R. Soc. Lond. B Biol. Sci. 371.
938 Veron J.E.N. 1995. Corals in Space and Time: The biogeography and evolution of the
939 Scleractinia. Cornell University Press New York.
940 Ward R.D., Holmes B.H., O'Hara T.D. 2008. DNA barcoding discriminates echinoderm
941 species. Mol. Ecol. Res. 8,1202-1211.
942 Wray G.A. 1996. Parallel evolution of nonfeeding larvae in echinoids. Syst. Biol. 45,308-
943 322.
944
945 **Figure Legends**
946
947 Fig. 1. Morphological variation in ophiocomid adults and larvae; University of Florida (UF)
948 and Museums Victoria (MV) specimen numbers in brackets. (A) *Ophiocoma* (=*Breviturma*)
949 *dentata*, Ningaloo Australia, ventral view (UF 9545) © F. Michonneau. (B) *Ophiocoma*
950 (=*Breviturma*) *pica*, Djibouti (UF 11975) © G. Paulay. (C) *Ophiomastix mixta* vitellaria
951 (lecithotrophic larva, orientated horizontally for convenience) © P. Cisternas. (D) *Ophiocoma*
952 *echinata* ophiopleuteus (planktotrophic larva) © P. Cisternas. (E) *Ophiomastix annulosa*,
953 Okinawa Japan (UF 10764) © G. Paulay. (F) *Ophiocomella sexradia*, Heron Island Australia
954 (UF 10095) © F. Michonneau. (G) *Ophiocoma scolopendrina* Samoa (MV F91612), arrow
955 indicates tooth papillae © G. Bribiesca-Contreras. (H) *Ophiocoma erinaceus* Ningaloo,
956 Australia (UF 9423) © F. Michonneau. (I) *Ophiarthrum (=Ophiomastix) pictum* Lizard
957 Island Australia (UF 8399) © F. Michonneau.
958
959 Fig. 2. Summary consensus phylogeny with new generic divisions. This tree is based on the
960 maximum Likelihood (RAxML) phylogeny of concatenated nuclear exon data (257kbp),
961 collapsing all nodes with <95% bootstrap or <0.95 ASTRAL-II Local Posterior Probability
962 support. Terminals are labelled with previous generic names showing the polyphyly of
963 *Ophiocoma* in particular, proposed generic names are to the right.
964
965 Fig. 3. BEAST concatenated exon and mtDNA super-matrix relaxed-clock chronogram.
966 Nodes are annotated with 95% HPD and posterior support where < 1.0. Terminals are

967 labelled with our new generic names and coloured by distribution (red= Atlantic, blue=East
968 Pacific, green=West Indian Ocean, black=East Indo-West Pacific).
969
970 Fig. 4. Allelic diversity in *Ophiocomella*. The fissiparous species are marked in red, other
971 related taxa in the clade marked in blue. (A) Number of alleles (sequences types) per locus
972 (80-150 genes per sample); virtually all loci assessed only had either one or two sequence
973 types, indicating that all samples are diploid. (B) Allelic divergence per locus (350-400 genes
974 per sample), indicating that the divergence between alleles is consistently higher in the
975 fissiparous samples. (C) StarBEAST2 gene trees, visualized using DensiTree (v2.01,
976 Bouckaert 2010), highlighting the gene tree diversity in the phased fissiparous samples. For
977 clarity only the *Ophiocomella* clade is shown; the full species tree is shown in Fig. S8.
978
979 Fig. 5. The effect of divergent *Ophiomastix flaccida* and *O. pictum* mitochondrial genes. (A)
980 PCoA of gene order differences (via a breakpoints and reversals distance matrix) showing the
981 divergence of *O. flaccida* from 7 previously published ophiuroid mitogenomes (Table S4).
982 (B) PCoA of mitochondrial COI base composition differences, showing how different *O.*
983 *flaccida* and *O. pictum* are to the rest of the Ophiocomidae and outgroups. (C) Optimal model
984 ML tree of Ophiocomidae COI illustrating the extreme inferred divergence of *O. flaccida* and
985 *O. pictum*. (D) Nuclear gene amino acid phylogeny of the Ophiocomidae, showing the
986 accelerated divergence of *O. flaccida* and *O. pictum* in the nuclear mitochondrial genes
987 compared to general cellular genes. For clarity only the *Ophiomastix* clade is shown, tree
988 heights are scaled to allow visual comparison.
989
990 Fig. 6. (A) First two axes of PCoA ordination of 36 morphological characters with symbols
991 indicating the new generic names. (B) Relative morphological disparity (MDI, indicated by
992 the size of the symbol, see Fig. S9) of each clade superimposed onto the Beast molecular
993 super-matrix chronogram (Fig. 3) with symbols on top representing the known presence of
994 three key life history innovations (Table 1).

Table 1. Developmental and larval characters for ophiocomids. Egg diameter - the mean size (+/-SE) of eggs from species spawned from this study, *- dissected from gravid ovaries, > - measured from premature eggs; Egg colour: G-green, B-burgundy; Developmental mode: L-lecithotrophic, P-planktotrophic, brackets-inferred from egg size; Larval type: O-ophiopluteus, V-vitellaria; Egg envelope: O-ornate, S-smooth; Region: GBR-Great Barrier Reef, NSW-New South Wales, WA-Western Australia; empty cells represent unknown values.

Species	Egg diameter (µm)	Egg buoyancy	Egg colour	Develop. Mode	Larval type	Egg envelope	Region	Reference
Breviturma brevipes	65 (2.3) n=20	-	B	(P)		S	GBR	This study
Breviturma dentata	75 (1.2) n=41	-	B	P	O	S	GBR	This study
Breviturma doederleini	80 (0.25) n=20	-	B	P		S	GBR	This study
Breviturma longispina	100* (0) n=20		B	(P)			Easter Is	This study
Breviturma pica		(+)		P	O	S	GBR	Mortensen (1937)
Breviturma pusilla	63 (2.9) n=20	-	B	P	O	S	GBR	This study
Ophiocoma aethiops	55 (0) n=25	-	B	P	O	O	Panama	This study
Ophiocoma anaglyptica	97* (0.9) n=20		B	(P)			GBR	This study
Ophiocoma echinata	81 (0.6) n=77	-	B	P	O	O	Panama	Mortensen (1921), (1937); this study
Ophiocoma erinaceus	91 (0.23) n=63	-	B	P	O	O	GBR	This study
Ophiocoma scolopendrina	100 (0.7) n=40	-	B	P	O	O	GBR	Mortensen (1937); Delroisse et al. (2013); this study
Ophiocoma schoenleinii	91 (2.0) n=61	-	B	P	O	O	GBR	This study
Ophiocomella alexandri	64 (0) n=50	-	B	P	O	S	Panama	This study
Ophiocomella ophiactoides	80			P	O	S	Caribbean	Mladenov and Emson (1984)
Ophiocomella pumila	73	-		P	O	S	Caribbean	Mladenov (1985)
Ophiomastix annulosa	430 (2.4) n=22	+	G	L	V	S	GBR	This study
Ophiomastix caryophyllata	> 200 (0) n=20	+	G	(L)			GBR	This study
Ophiomastix elegans	384 (1.8) n=66	+	G	L	V		GBR	This study
Ophiomastix endeani	> 342 (2.3) n=23		G	(L)		S	NSW	This study
Ophiomastix janualis	> 200 (0) n=20		G	(L)			GBR	This study
Ophiomastix macroplaca	100* (0) n=20		B	(P)			Hawaii	This study
Ophiomastix marshallensis	> 224* (3.3) n=20		G	(L)			Marshall Is	This study
Ophiomastix mixta	335 (3.3) n=20	+	G	L	V	S	GBR	This study
Ophiomastix occidentalis	66* (1.0) n=22		B	(P)			WA	This study
Ophiomastix pictum	419 (3.4) n=46	+	G	L	V	S	GBR	This study
Ophiomastix venosa	550	+	G	L	V	S	Madagascar	Fourgon et al. (2005)
Ophiomastix wendtii	100 (0.2) n=50	-	B	P	O	S	Panama	This study

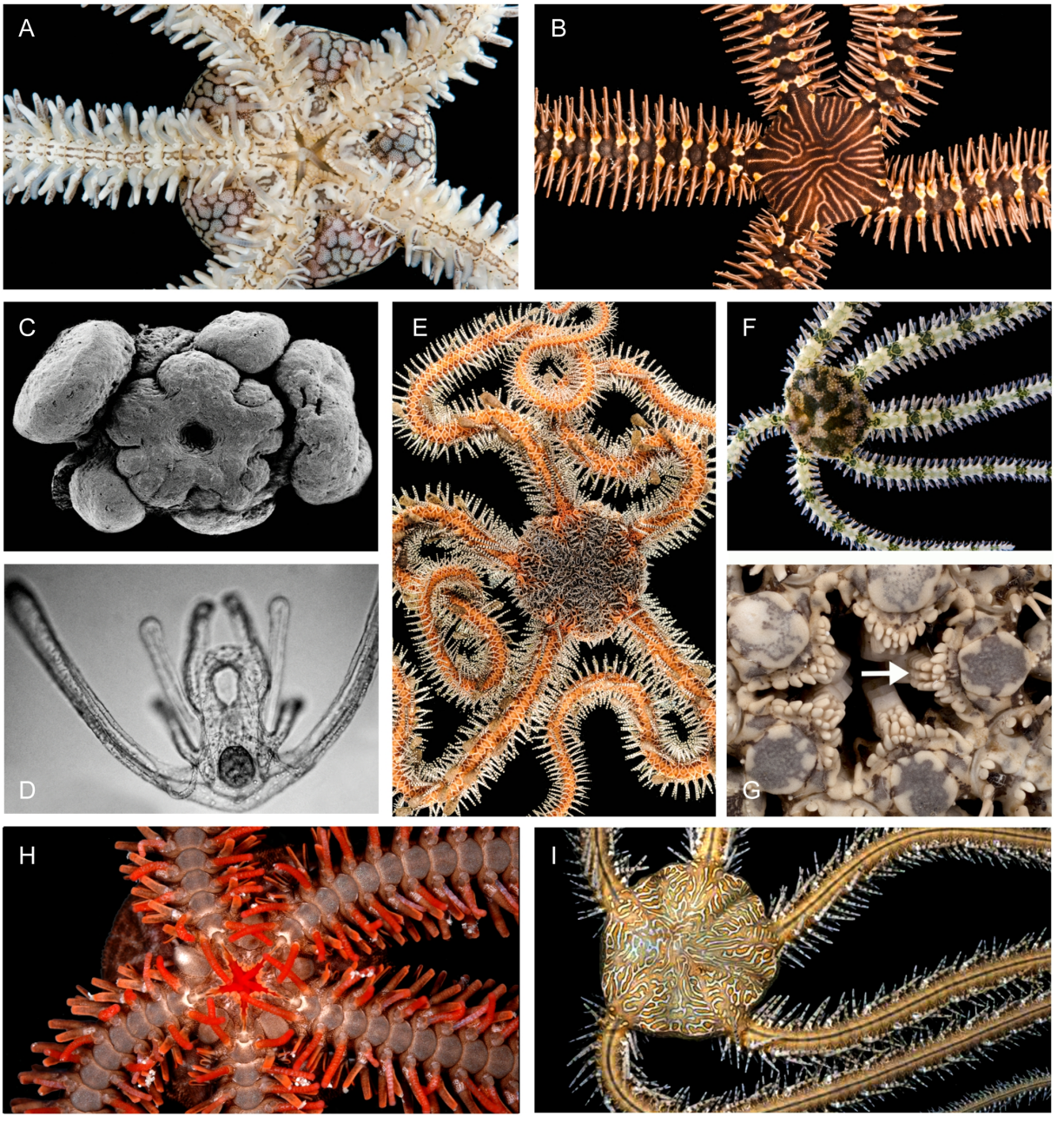
A
B
C
E
F
D
G
H
I

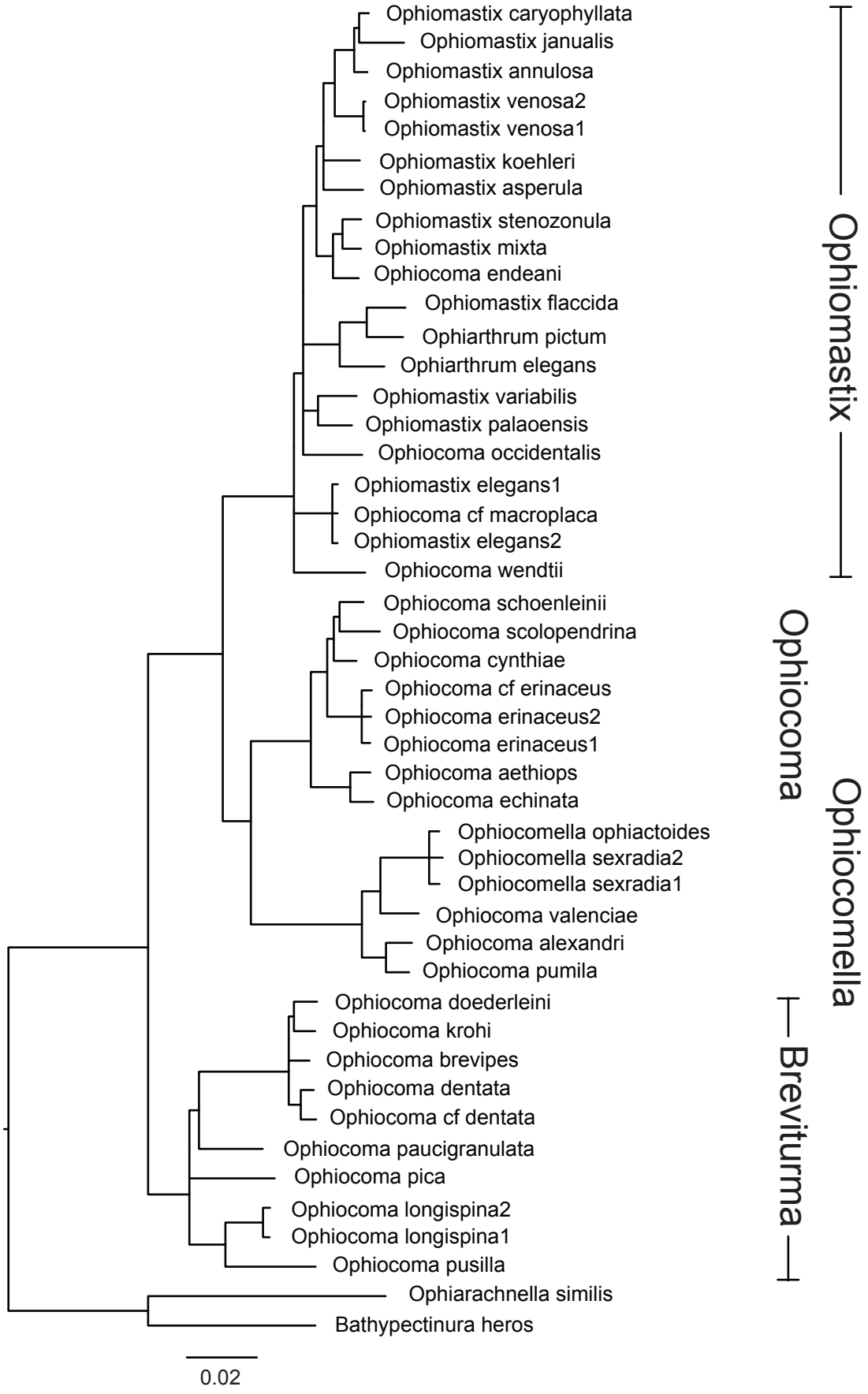
Ophiomastix caryophyllata
Ophiomastix janualis
Ophiomastix annulosa
Ophiomastix venosa2
Ophiomastix venosa1
Ophiomastix koehleri
Ophiomastix asperula
Ophiomastix stenozonula
Ophiomastix mixta
Ophiocoma endeani
Ophiomastix flaccida
Ophiarthrum pictum
Ophiarthrum elegans
Ophiomastix variabilis
Ophiomastix palaoensis
Ophiocoma occidentalis
Ophiomastix elegans1
Ophiocoma cf macroplaca
Ophiomastix elegans2
Ophiocoma wendtii
Ophiocoma schoenleinii
Ophiocoma scolopendrina
Ophiocoma cynthiae
Ophiocoma cf erinaceus
Ophiocoma erinaceus2
Ophiocoma erinaceus1
Ophiocoma aethiops
Ophiocoma echinata
Ophiocomella ophiactoides
Ophiocomella sexradia2
Ophiocomella sexradia1
Ophiocoma valenciae
Ophiocoma alexandri
Ophiocoma pumila
Ophiocoma doederleini
Ophiocoma krohi
Ophiocoma brevipes
Ophiocoma dentata
Ophiocoma cf dentata
Ophiocoma paucigranulata
Ophiocoma pica
Ophiocoma longispina2
Ophiocoma longispina1
Ophiocoma pusilla
Ophiarachnella similis
Bathypectinura heros
0.02
Ophiomastix
Ophiocoma
Ophiocomella
Breviturma

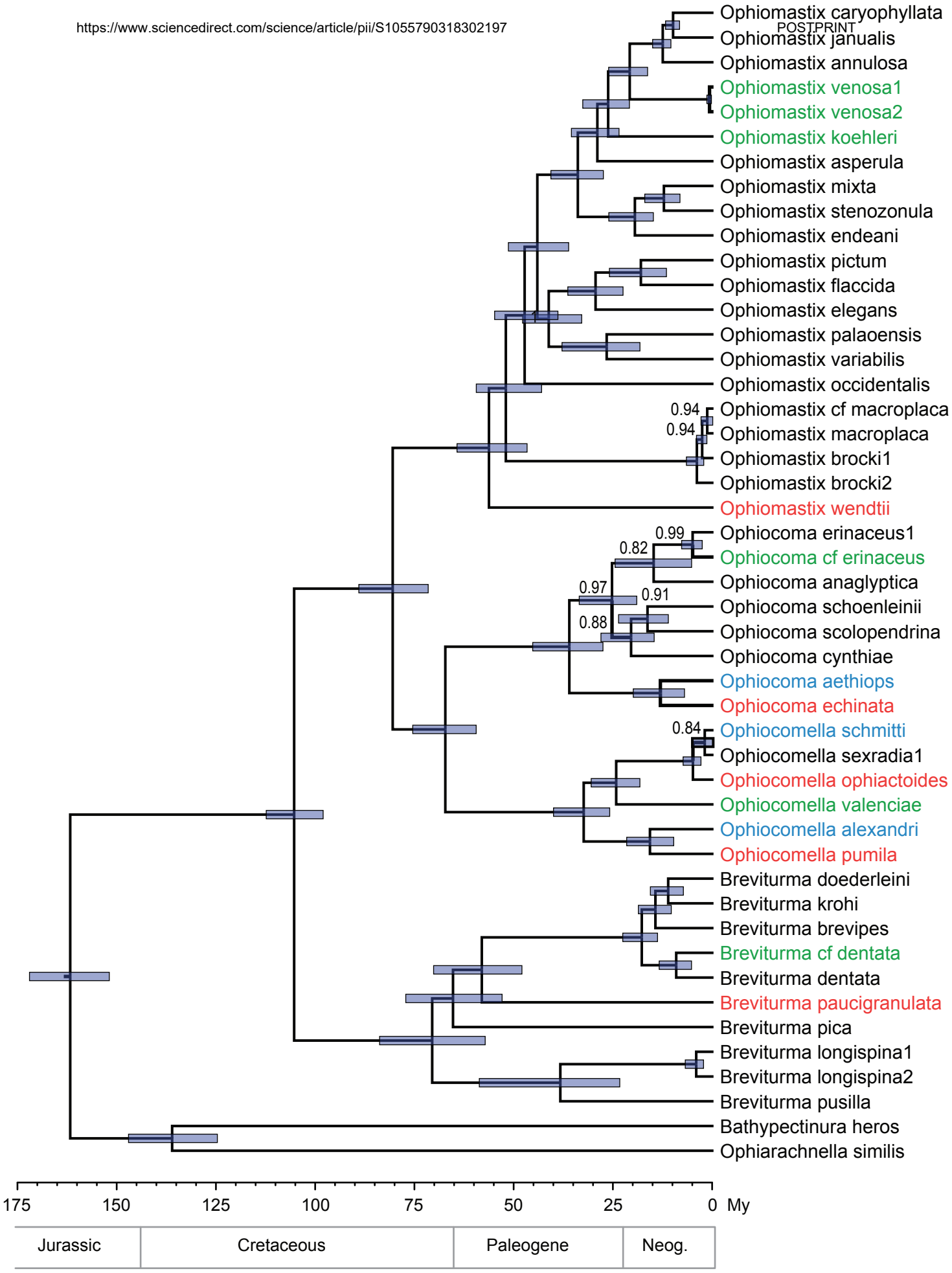

A Number of alleles per locus

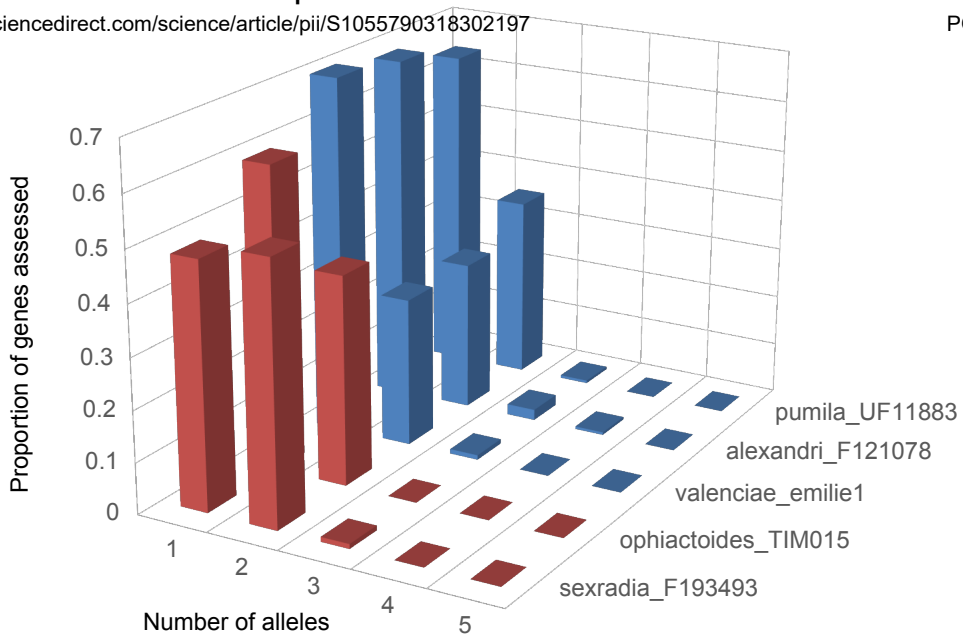

B Allellic divergence per locus

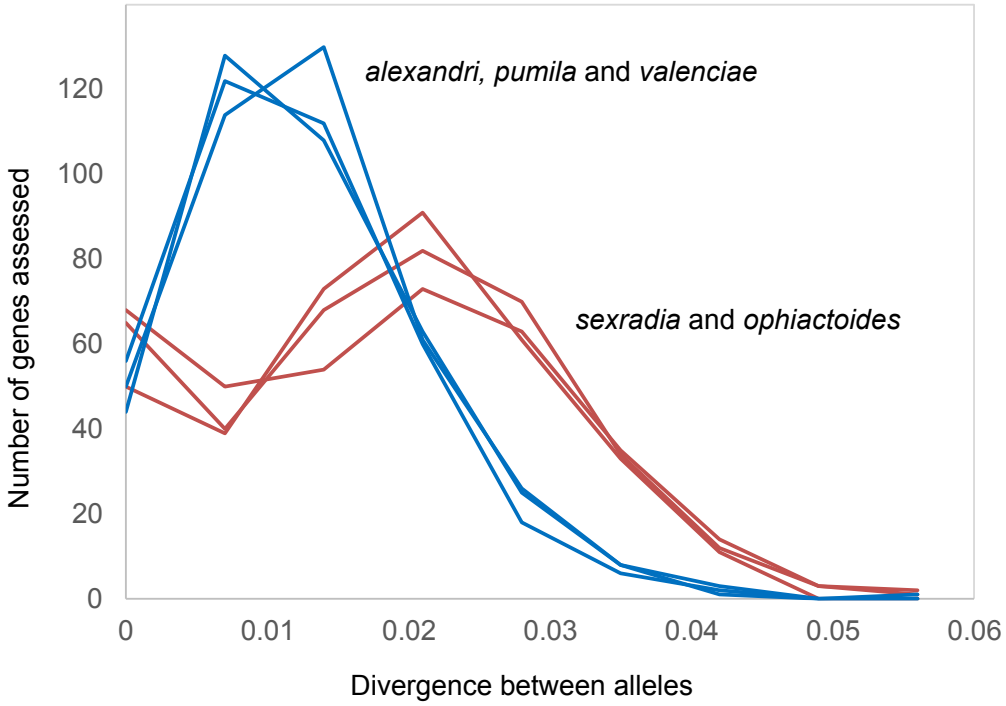

C StarBEAST gene trees

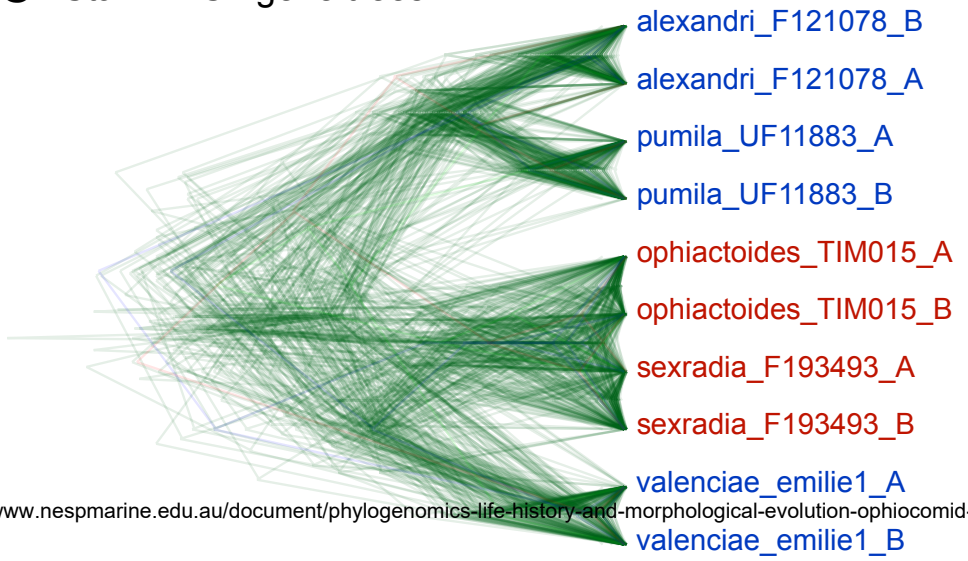

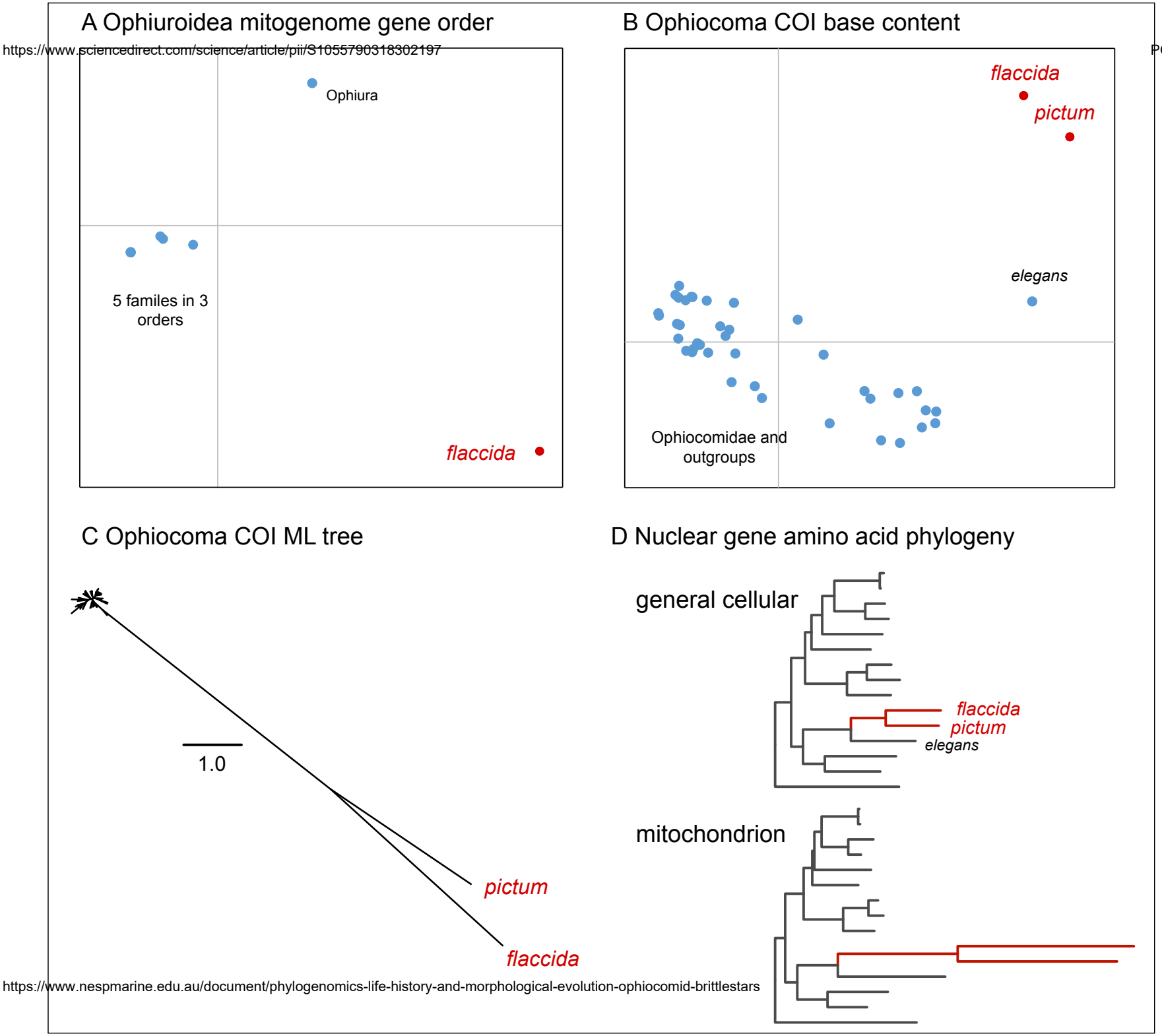

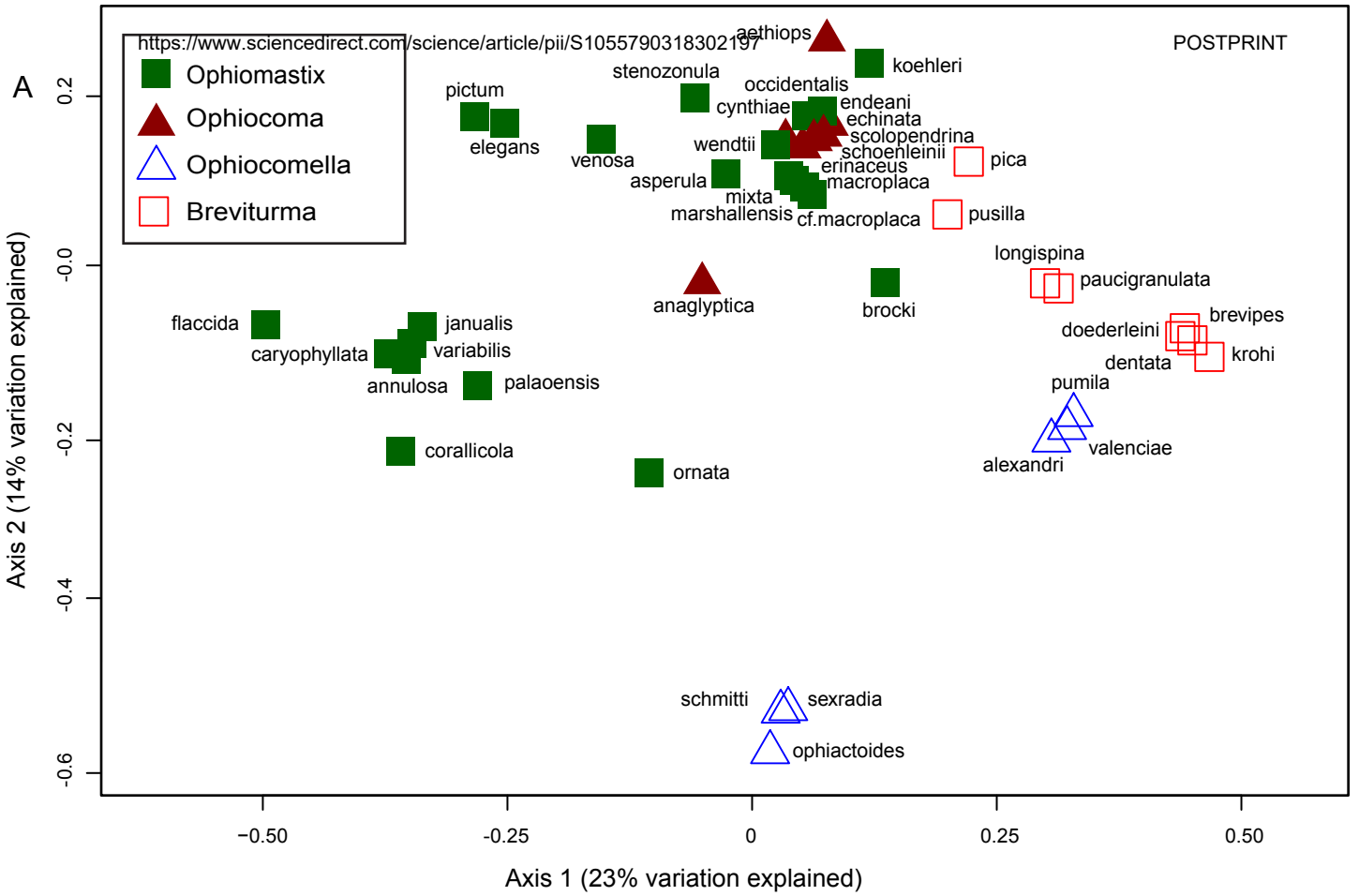

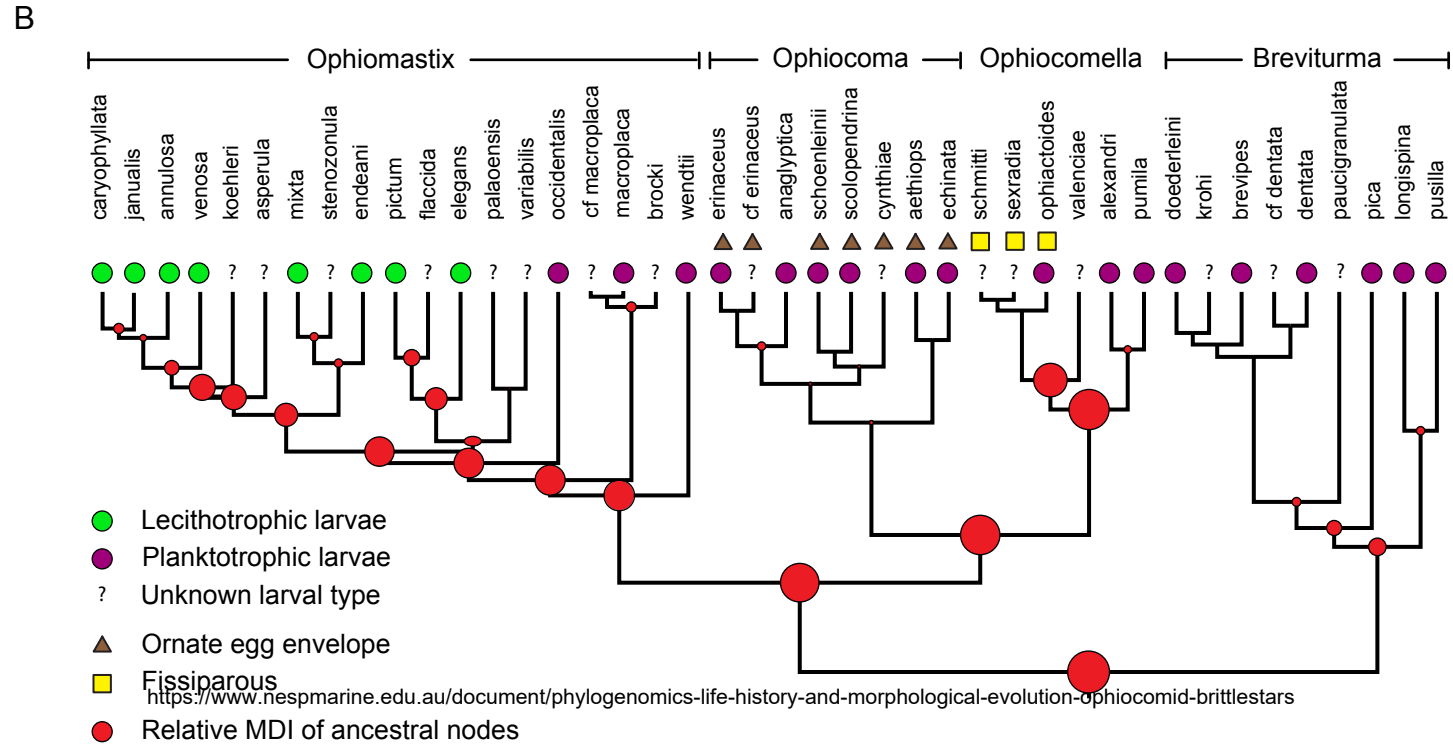

Appendix A: Supplementary Information

Phylogenomics, life history and morphological evolution of ophiocomid brittlestars

Timothy D. O'Hara [a], Andrew F. Hugall [a], Paula A. Cisternas [b], Emilie Boissin [c], Guadalupe Bribiesca-Contreras [a,d], Javier Sellanes [e], Gustav Paulay [f], Maria Byrne [b]

[a] *Museums Victoria, Sciences Department, GPO Box 666, Melbourne, 3000, Australia*

[b] *University of Sydney, School of Medicine, Discipline of Anatomy and Histology, 2006, Australia*

[c] *PSL Research University: EPHE-UPVD-CNRS, USR 3278 CRIOBE, Université de Perpignan, Laboratoire d'Excellence CORAIL, 52 Avenue Paul Alduy, 66860 Perpignan Cedex, France*

[d] *University of Melbourne, Biosciences, 3010, Australia*

[e] *Universidad Católica del Norte, Departamento de Biologia Marina, Coquimbo, Chile*

[f] *University of Florida, Florida Natural History Museum, Gainesville, USA*

Table S1 and S2 are in separate Excel spreadsheet files

Table S1. List of samples in phylogenetic analyses, including sequences obtained from exon-capture (EC) (Hugall et al. 2016; O'Hara et al. 2017); transciptomes (T) (O'Hara et al., 2014) and Sanger sequencing (S). For some taxa, the 16S sequence was obtained from a separate specimen than the exon-capture or transcriptomic one.

Table S2. Morphological character matrix for adult ophiocomid species, with raw data and the state transformation (in brackets) for quantitative analysis. Character types: b = binary (0, 1), m = unordered multistate (0-6), o = ordered multistate (0-6), q = quantitative (mean) (0-6); ? = missing data, -= not applicable.

Table S3. Normalised PCoA species scores on 5 axes. These scores were used to generate the Morphological Disparity Indices (Fig. S9).

Species	Genus (prior)	Genus (new)	Axis 1	Axis 2	Axis 3	Axis 4	Axis 5
aethiops	*Ophiocoma*	*Ophiocoma*	0.195	-1.968	0.488	0.177	-1.729
alexandri	*Ophiocoma*	*Ophiocomella*	3.826	1.586	-2.808	1.635	2.309
anaglyptica	*Ophiocoma*	*Ophiocoma*	-1.455	-1.015	1.408	9.122	-3.898
annulosa	*Ophiomastix*	*Ophiomastix*	-5.543	0.812	-1.425	1.095	3.744
asperula	*Ophiomastix*	*Ophiomastix*	-1.075	-1.580	0.901	0.492	1.142
brevipes	*Ophiocoma*	*Breviturma*	5.187	1.063	-3.631	-0.437	-0.280
brocki	*Ophiomastix*	*Ophiomastix*	0.396	-0.286	-0.242	0.047	0.037
caryophyllata	*Ophiomastix*	*Ophiomastix*	-4.831	0.870	-1.101	1.542	3.076
cf *macroplaca*	*Ophiocoma*	*Ophiomastix*	0.467	-1.611	1.742	-0.426	0.225
corallicola	*Ophiomastix*	*Ophiomastix*	-3.298	1.927	-1.024	0.178	0.768
cynthiae	*Ophiocoma*	*Ophiocoma*	-0.444	-2.317	1.054	-0.698	0.520
dentata	*Ophiocoma*	*Breviturma*	5.158	0.746	-3.079	0.003	-0.314
doederleini	*Ophiocoma*	*Breviturma*	5.392	0.896	-3.006	-0.054	-0.867
echinata	*Ophiocoma*	*Ophiocoma*	0.454	-2.212	1.515	-0.353	0.082
elegans	*Ophiarthrum*	*Ophiomastix*	-3.136	-0.460	-1.934	-1.534	-4.793
endeani	*Ophiocoma*	*Ophiomastix*	-0.150	-2.949	0.822	-0.896	0.596
erinaceus	*Ophiocoma*	*Ophiocoma*	0.025	-2.474	1.896	0.491	1.161
flaccida	*Ophiomastix*	*Ophiomastix*	-5.391	1.572	-1.543	-1.599	-1.278
janualis	*Ophiomastix*	*Ophiomastix*	-5.431	0.952	-2.760	0.582	2.656
koehleri	*Ophiomastix*	*Ophiomastix*	0.500	-1.762	0.847	-0.742	-0.097
krohi	*Ophiocoma*	*Breviturma*	5.357	1.193	-3.292	-1.216	-1.138
longispina	*Ophiocoma*	*Breviturma*	3.424	-0.571	1.323	-0.267	-0.658
macroplaca	*Ophiocoma*	*Ophiomastix*	0.467	-1.611	1.742	-0.426	0.225
marshallensis	*Ophiomastix*	*Ophiomastix*	0.202	-1.110	0.363	-0.616	0.296
mixta	*Ophiomastix*	*Ophiomastix*	-0.023	-1.676	0.630	-0.177	0.713
occidentalis	*Ophiocoma*	*Ophiomastix*	0.147	-2.342	1.387	-0.430	0.123
ophiactoides	*Ophiocomella*	*Ophiocomella*	-0.001	6.382	3.642	0.100	0.027
ornata	*Ophiomastix*	*Ophiomastix*	-1.230	1.084	0.306	-1.471	-0.251
palaoensis	*Ophiomastix*	*Ophiomastix*	-3.363	1.741	-1.256	-0.882	-0.013
paucigranulata	*Ophiocoma*	*Breviturma*	3.169	-1.317	1.936	1.115	1.509
pica	*Ophiocoma*	*Breviturma*	2.862	-1.965	1.900	-0.439	0.830
pictum	*Ophiarthrum*	*Ophiomastix*	-3.349	-0.650	-1.929	-0.713	-4.200
pumila	*Ophiocoma*	*Ophiocomella*	3.474	1.185	-2.865	-0.206	0.265
pusilla	*Ophiocoma*	*Breviturma*	2.605	-0.432	3.742	-0.932	-0.243
schmitti	*Ophiocomella*	*Ophiocomella*	0.686	7.158	3.860	-0.528	-0.497
schoenleinii	*Ophiocoma*	*Ophiocoma*	0.106	-1.992	1.642	-0.422	-0.102
scolopendrina	*Ophiocoma*	*Ophiocoma*	0.117	-2.061	0.893	-0.948	-0.135
sexradia	*Ophiocomella*	*Ophiocomella*	0.686	7.158	3.860	-0.528	-0.497
stenozonula	*Ophiomastix*	*Ophiomastix*	-0.895	-0.960	-1.271	-0.391	0.005
valenciae	*Ophiocoma*	*Ophiocomella*	3.347	1.306	-3.069	2.631	1.681
variabilis	*Ophiomastix*	*Ophiomastix*	-4.701	1.835	-1.922	-0.184	-1.409
venosa	*Ophiomastix*	*Ophiomastix*	-3.514	-2.104	-0.749	-1.879	-0.191
wendtii	*Ophiocoma*	*Ophiomastix*	-0.417	-2.044	1.005	0.185	0.599

Table S4. Mitogenome gene order information. Sequence data from either GenBank (accession) or *de novo* assembled (sample ID code) from exon-capture.

Taxon	**Family**	**Order**	**GenBank**	***de novo***
Amphipholis squamata	Amphiuridae	Amphilepidida	FN562578	
Ophiopholis aculeata	Ophiopholidae	Amphilepidida	AF314589.1	
Astrospartus mediterraneus	Gorgonocephalidae	Euryalida	FN562580	
Ophiacantha lineata	Ophiacanthidae	Ophiacanthida	KC990833	
Ophiocomina nigra	Ophiotretidae	Ophiacanthida	FN562577	
Ophiura lutkeni	Ophiopyrgidae	Ophiurida	AY184223	
Ophiura albida	Ophiuridae	Ophiurida	AM404180	
Ophiomastix flaccida	Ophiocomidae	Ophiacanthida	TBD	UF15654a

Imputed *Ophiomastix flaccida* mitogenome gene order used for CREx analysis. Gene orders for all taxa were determined by MITOS and linear list set to start with COI, coding strand. Figure shows MITOS gene map for the 16,747 base Trinity assembled contig.

Ophiomastix_flaccida_UF15654a cox1 trnN nad2 trnF cox3 trnR trnT cob atp8 trnD nad4 trnI nad5 trnY trnW nad1 trnS1 trnM trnQ rrnL trnG trnC rrnS trnP trnL1 trnA trnL2 nad6 trnH nad3 trnK trnS2 cox2 trnV nad4l atp6 trnE

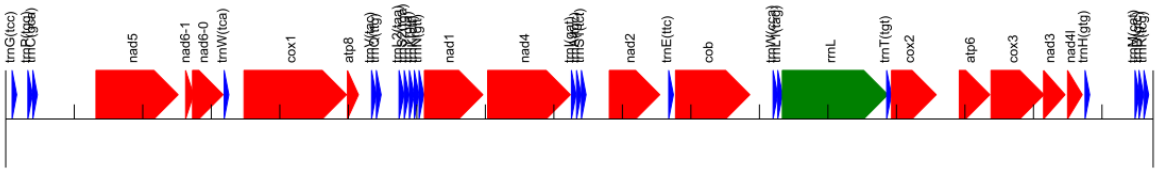

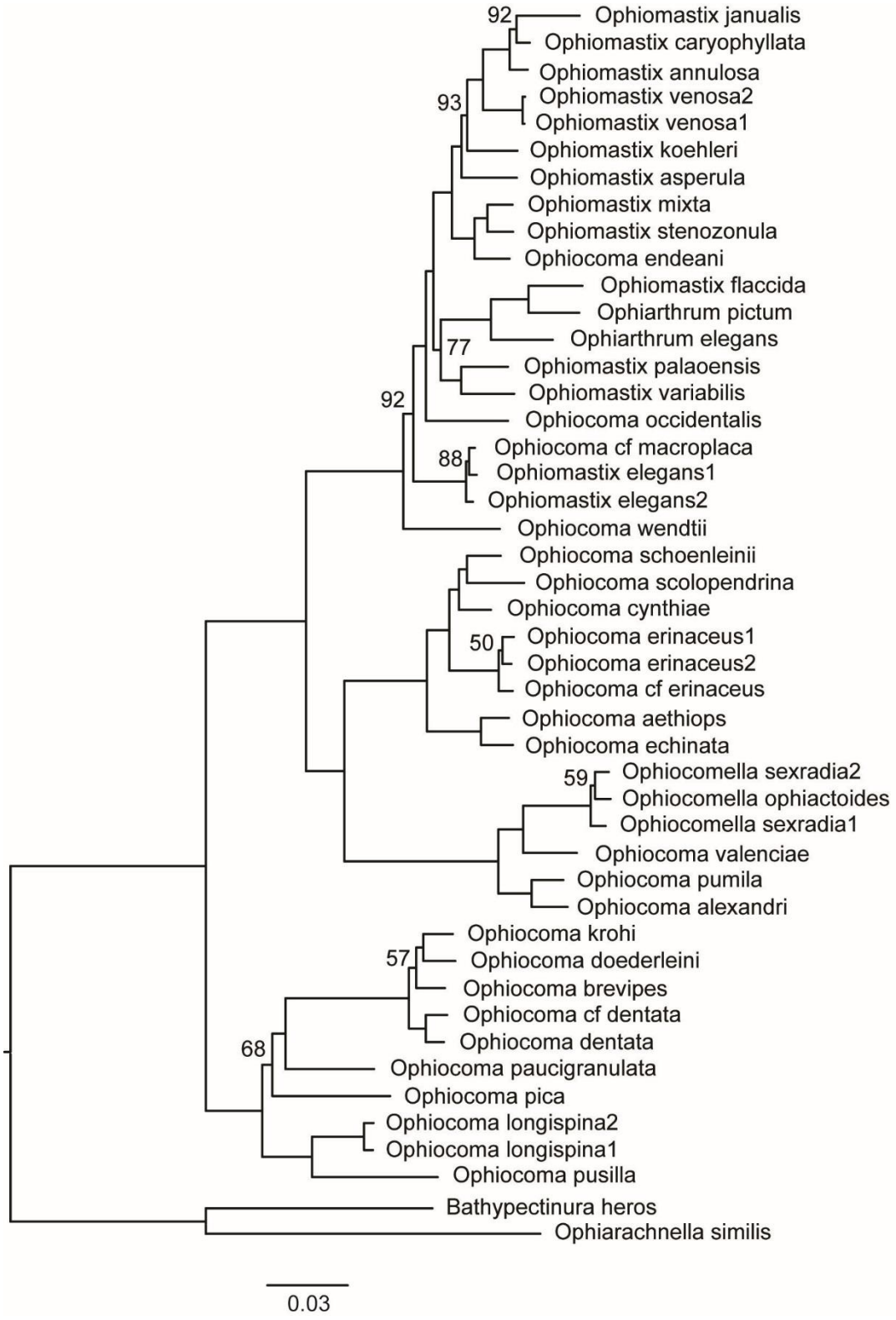

Fig. S5. Maximum Likelihood (RAxML) phylogeny of concatenated nuclear exon data (257kbp), partitioned by colon position, using a GTRGAMMA model. Only nodes with less than 100% bootstrap support (n=200) are indicated. Labelled with the previous generic names (Table S1).

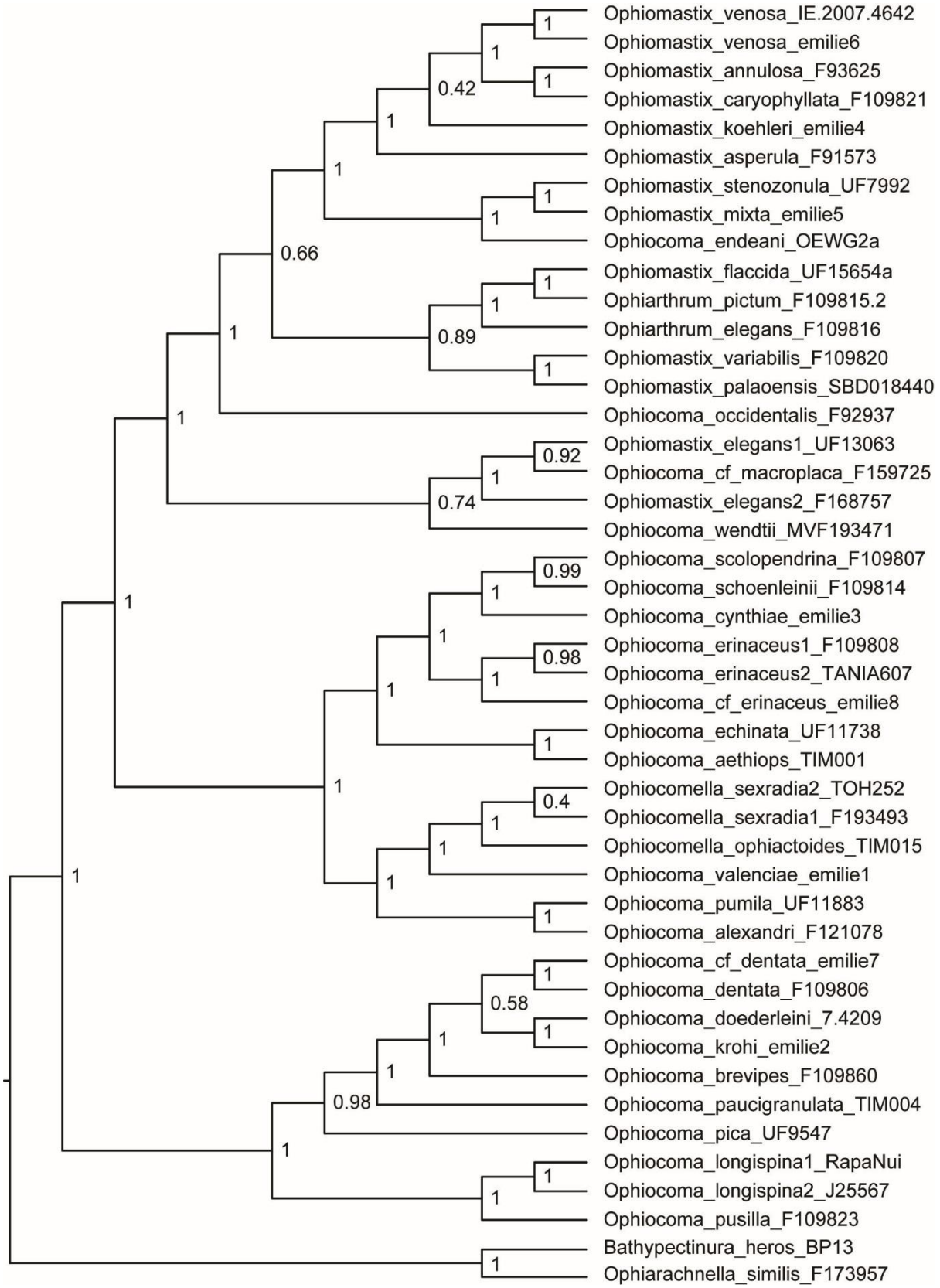

Fig. S6. ASTRAL-II species tree of nuclear exon data, derived from 339 RAxML single-gene trees, with local posterior support. Labelled with the previous generic names and sample code (Table S1). *Ophiomastix janualis* and *Ophiocomella schmitti* were omitted due to low coverage.

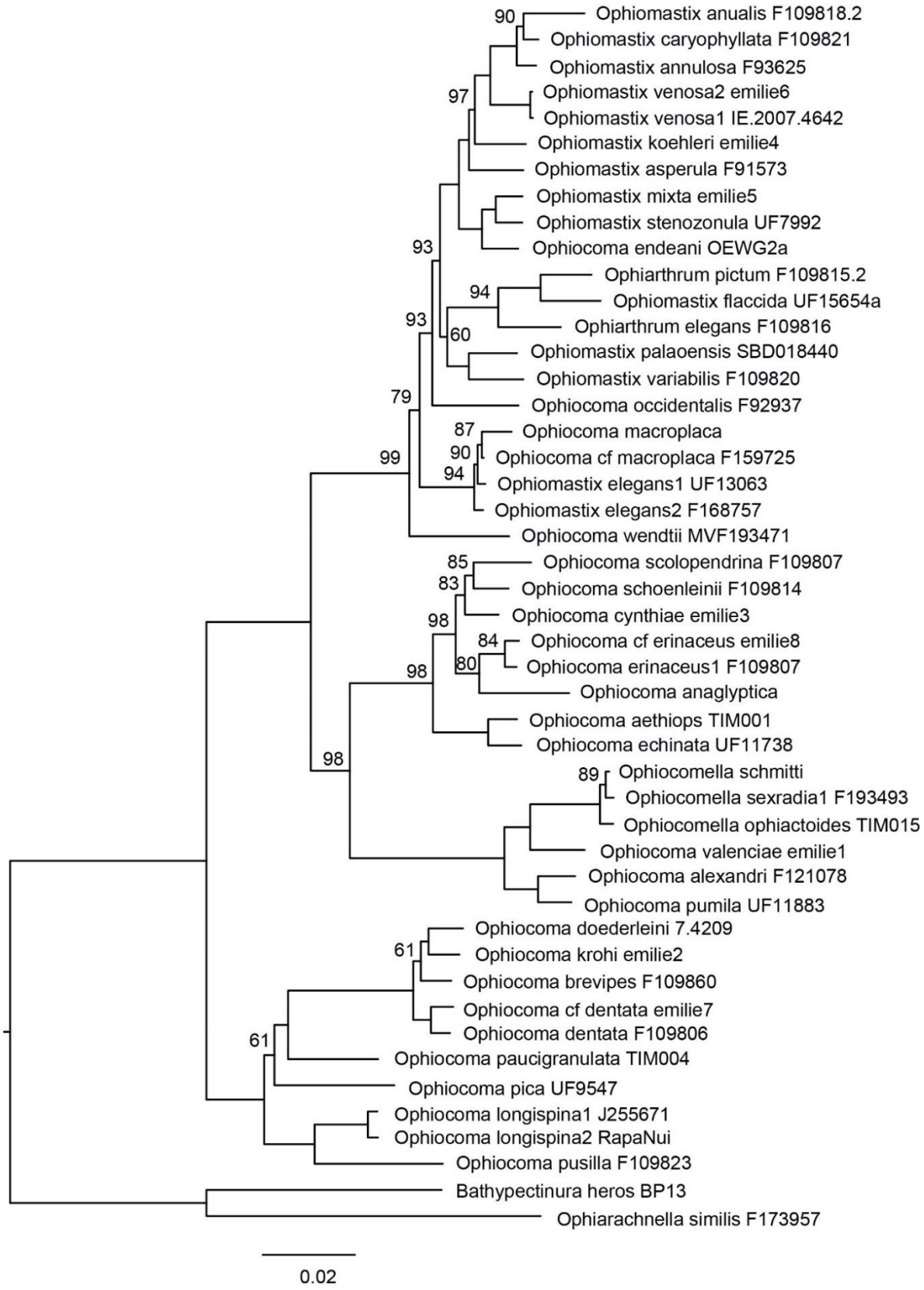

Fig. S7. RAxML analysis of the super-matrix (4 partitions: 3 codon-position exon data and COI+16S), using a GTR+Γ, with bootstrap support (n=200, 100% support not shown). Labelled with the previous generic names and sample code (Table S1).

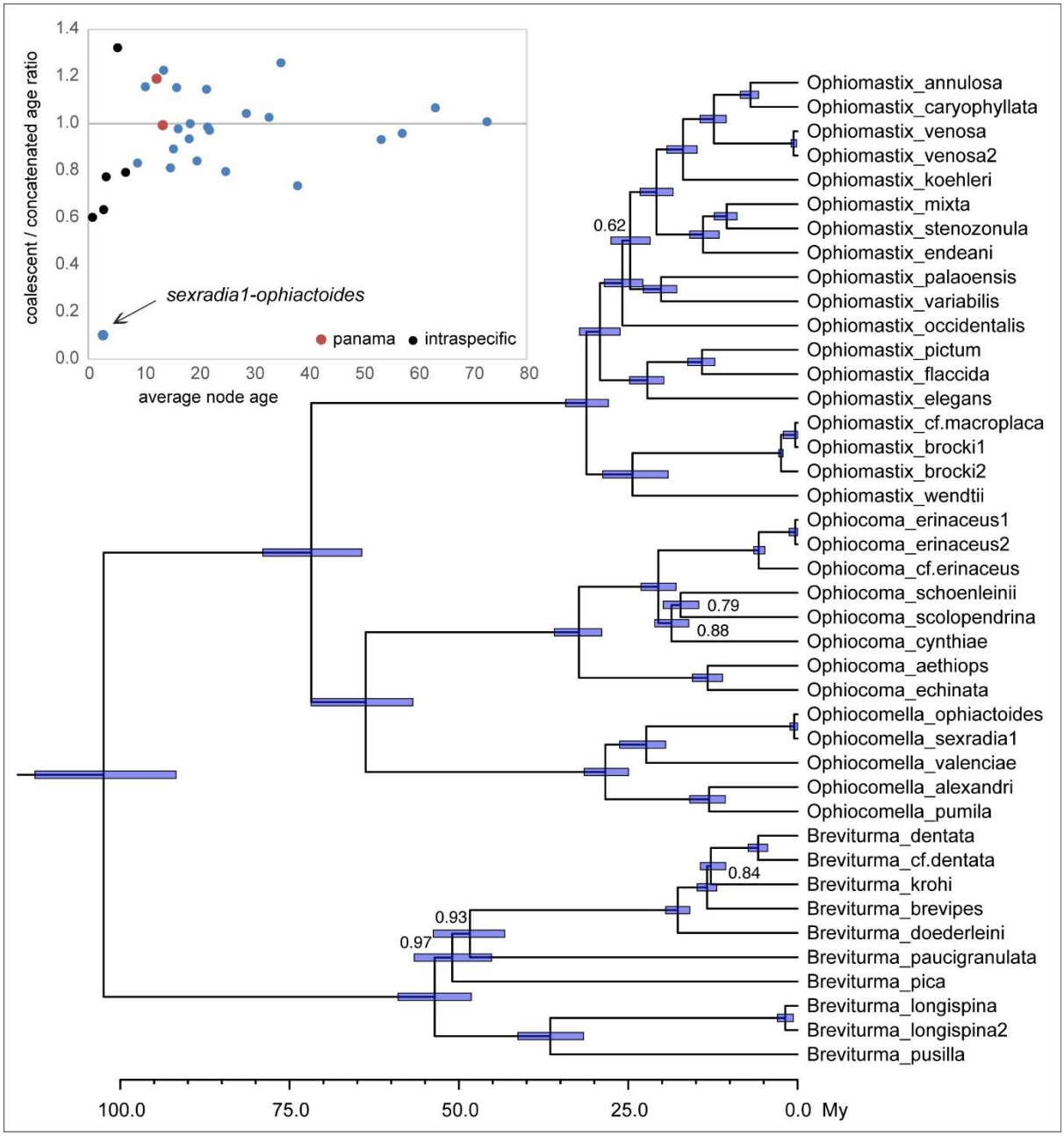

Fig. S8. StarBEAST2 coalescent-based species tree and comparison of divergence age estimation with concatenated data (inset). Divergence age estimates are essentially the same for the putative Panamanian geminate species pairs (*Ophiocoma aethops-echinata* and *Ophiocomella alexandri-pumila*) but very different for the fissiparous species *O. sexradia-ophiactoides*. Tree labelled with the new generic names, node age 95% HPD and posterior support where <1.0.

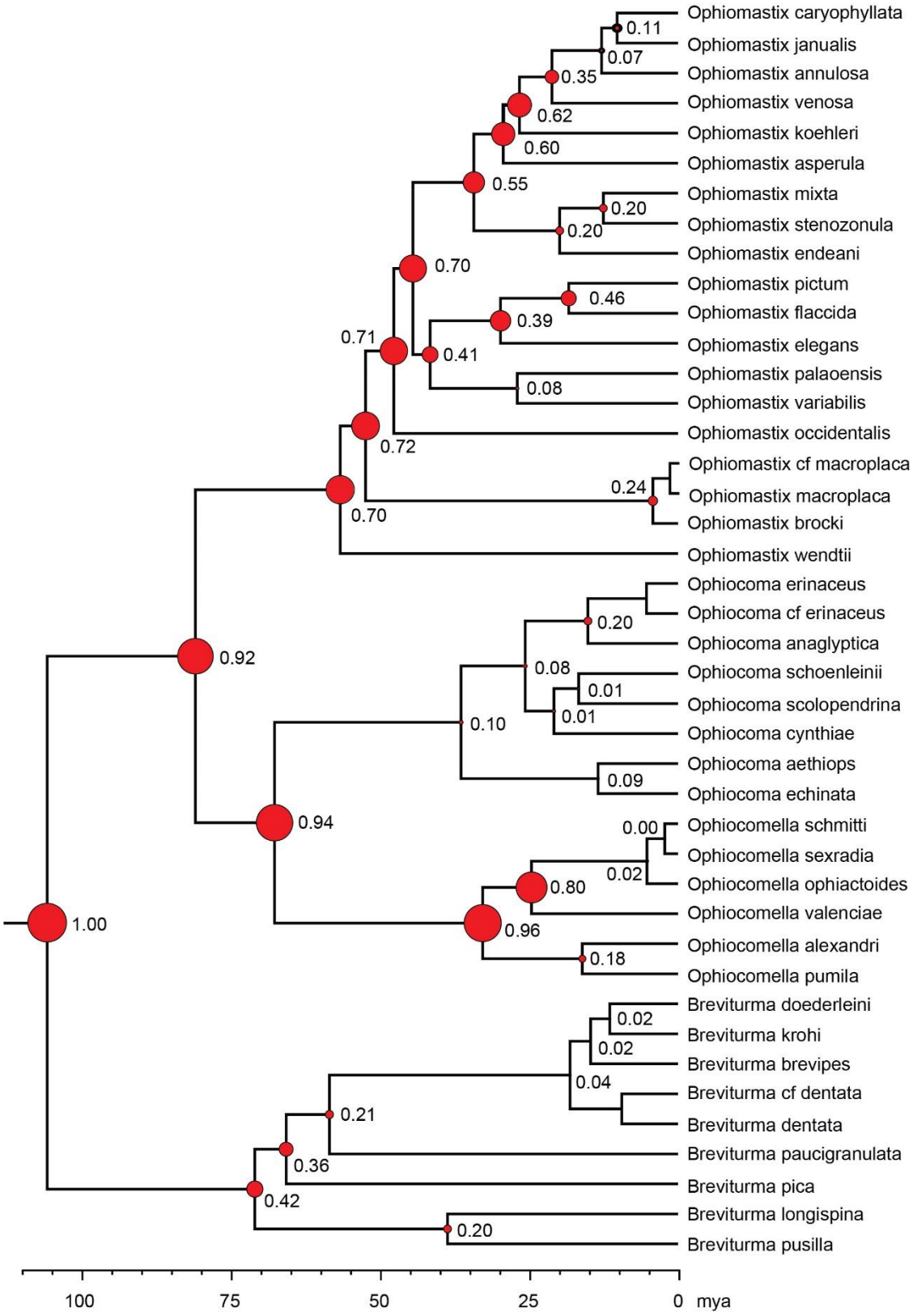

Fig. S9. The relative morphological disparity (Harmon et al. 2003) of each clade superimposed (via node label and symbol size) onto the Beast molecular super-matrix chronogram. Labelled with the new generic names.